Match-up database Analyses Report

SMAP SSS L3 v4 - Monthly (RSS)

Waveglider

SPURS 2

prepared by the Pi-MEP Consortium

June 15, 2022

Contents

List of Figures

Acronym

Aquarius	NASA/CONAE Salinity mission
ASCAT	Advanced Scatterometer
ATBD	Algorithm Theoretical Baseline Document
BLT	Barrier Layer Thickness
CMORPH	CPC MORPHing technique (precipitation analyses)
CPC	Climate Prediction Center
CTD	Instrument used to measure the conductivity, temperature, and pressure of seawater
DM	Delayed Mode
EO	Earth Observation
ESA	European Space Agency
FTP	File Transfer Protocol
GOSUD	Global Ocean Surface Underway Data
GTMBA	The Global Tropical Moored Buoy Array
Ifremer	Institut français de recherche pour l'exploitation de la mer
IPEV	Institut polaire français Paul-Émile Victor
IQR	Interquartile range
ISAS	*In Situ* Analysis System
Kurt	Kurtosis (fourth central moment divided by fourth power of the standard deviation)
L2	Level 2
LEGOS	Laboratoire d'Etudes en Géophysique et Océanographie Spatiales
LOCEAN	Laboratoire d'Océanographie et du Climat : Expérimentations et Approches Numériques
LOPS	Laboratoire d'Océanographie Physique et Spatiale
MDB	Match-up Data Base
MEOP	Marine Mammals Exploring the Oceans Pole to Pole
MLD	Mixed Layer Depth
NCEI	National Centers for Environmental Information
NRT	Near Real Time
NTAS	Northwest Tropical Atlantic Station
OI	Optimal interpolation
Pi-MEP	Pilot-Mission Exploitation Platform
PIRATA	Prediction and Researched Moored Array in the Atlantic
QC	Quality control
R_{sat}	Spatial resolution of the satellite SSS product
RAMA	Research Moored Array for African-Asian-Australian Monsoon Analysis and Prediction
r^2	Square of the Pearson correlation coefficient
RMS	Root mean square
RR	Rain rate
SAMOS	Shipboard Automated Meteorological and Oceanographic System
Skew	Skewness (third central moment divided by the cube of the standard deviation)
SMAP	Soil Moisture Active Passive (NASA mission)
SMOS	Soil Moisture and Ocean Salinity (ESA mission)
SPURS	Salinity Processes in the Upper Ocean Regional Study
SSS	Sea Surface Salinity
SSS_{insitu}	*In situ* SSS data considered for the match-up

SSS_{SAT}	Satellite SSS product considered for the match-up
ΔSSS	Difference between satellite and *in situ* SSS at colocalized point ($\Delta SSS = SSS_{SAT}$- SSS_{insitu})
SST	Sea Surface Temperature
Std	Standard deviation
Std*	Robust Standard deviation = median(abs(x-median (x)))/0.67 (less affected by outliers than Std)
Stratus	Surface buoy located in the eastern tropical Pacific
Survostral	SURVeillance de l'Océan AuSTRAL (Monitoring the Southern Ocean)
TAO	Tropical Atmosphere Ocean
TSG	ThermoSalinoGraph
WHOI	Woods Hole Oceanographic Institution
WHOTS	WHOI Hawaii Ocean Time-series Station
WOA	World Ocean Atlas

1 Overview

In this report, we present systematic analyses of the Match-up DataBase (MDB) files generated by the Pi-MEP platform within the following Pi-MEP region and for the below pair of Satellite/*in situ* SSS data:

- Pi-MEP region: SPURS 2 (download the corresponding mask in NetCDF here)

- SSS satellite product (SSS_{SAT}): SMAP SSS L3 v4 - Monthly (RSS)

- *In situ* dataset (SSS_{Insitu}): Waveglider (download the corresponding *in situ* report here)

In the following, $\Delta SSS = SSS_{SAT} - SSS_{Insitu}$ denotes the difference between the satellite and *in situ* SSS at the colocalized points that form the MDB.

This report presents successively:

The MDB file DataSets (Section 2)

- A short description of the satellite SSS product considered in the match-up (2.1)

- A short description of the *in situ* SSS dataset considered in the match-up (2.2)

- A short description of the auxiliary geophysical datasets co-localized with SSS pairs (2.3)

- An overview of how the Match-ups were evaluated (2.4)

- An overview of the MDB characteristics for the particular *in situ*/satellite pairs (2.5)

The major results of the MDB file Analyses (Section 3)

- Spatial Maps of the Time-mean and temporal Std of *in situ* and satellite SSS and of the ΔSSS (3.1)

- Time series of the monthly median and Std of *in situ* and satellite SSS and of the ΔSSS (3.2)

- Zonal mean and Std of *in situ* and satellite SSS and of the ΔSSS (3.3)

- Scatterplots of satellite vs *in situ* SSS by latitudinal bands (3.4)

- Time series of the monthly median and Std of the ΔSSS sorted by latitudinal bands (3.5)

- ΔSSS sorted as function of geophysical parameters (3.6)

- ΔSSS maps and statistics for different geophysical conditions (3.7)

All analyses are conducted over the Pi-MEP Region specified above and over the full satellite SSS product period. Original figures appearing in this report can be downloaded as PNG files here or by clicking directly on the figure.

2 The MDB file datasets

2.1 Satellite SSS product

2.1.1 SMAP SSS L3 v4 - Monthly (RSS)

The version 4.0 SMAP-SSS level 3, monthly gridded product is based on the fourth release of the validated standard mapped sea surface salinity (SSS) data from the NASA Soil Moisture Active Passive (SMAP) observatory, produced operationally by Remote Sensing Systems (RSS) with a one-month latency. Enhancements with this release include: use of an improved 0.125 degree land correction table with land emission based on SMAP TB; replacement of the previous NCEP sea-ice mask with one based on RSS AMSR-2 and implementing a sea-ice threshold of 0.3% (gain weighted sea-ice fraction); revised solar flagging that depends on glint angle and wind speed; inclusion of estimated SSS-uncertainty; consolidation of both 40 km and 70 km SMAP-SSS datasets as variable fields in a single data product. Monthly data files for this product are averages over one-month time intervals. SMAP data begins on April 1,2015 and is ongoing, with a one-month latency in processing and availability. L3 products are global in extent and gridded at 0.25° x 0.25° with a default spatial feature resolution of approximately 70 km. Note that while a SSS 40 km variable is also included in the product, for most open ocean applications, the default SSS variable (70 km) is best used as they are significantly less noisy than the 40 km data. The SMAP satellite is in a near-polar orbit at an inclination of 98 degrees and an altitude of 685 km. It has an ascending node time of 6 pm and is sun-synchronous. With its 1000 km swath, SMAP achieves global coverage in approximately 3 days, but has an exact orbit repeat cycle of 8 days. On board instruments include a highly sensitive L-band radiometer operating at 1.41 GHz and an L-band 1.26 GHz radar sensor providing complementary active and passive sensing capabilities. Malfunction of the SMAP scatterometer on 7 July, 2015, has necessitated the use of collocated wind speed, primarily from WindSat, for the surface roughness correction required for the surface salinity retrieval.

We only select data in the Match-up files such as the following conditions are met:

- the gain weighted land fraction $gland$ do not exceed 0.04 (4%)

- the land contamination fraction $fland$ do not exceed 0.001 (0.1%)

- the gain weighted sea ice fraction $gice$ do not exceed 0.003 (0.3%)

Table 1: Satellite SSS product characteristics

SMAP SSS L3 v4 - Monthly (RSS)	
Spatial resolution	~70 km gridded at 0.25° x 0.25°
Temporal resolution	1 Month
Temporal coverage	From 2015-03-27 to now
Spatial coverage	Global [-180 180 -90 90]
Data Provider	Remote Sensing Systems (RSS), Santa Rosa, USA
Release Date	2019-08-28
Version	4
User Guide	RSS_SMAP-SSS_V4.0_TechnicalDocumentation.pdf
Documentation	https://podaac-tools.jpl.nasa.gov/drive/files/allData/smap/docs/V4/
DOI	http://doi.org/10.5067/SMP40-3SMCS
Data access	http://www.remss.com/missions/smap/
Reference	Meissner et al. (2018)

2.2 *In situ* SSS dataset

A Waveglider is an autonomous platform propelled by the conversion of ocean wave energy into forward thrust and employing solar panels to power instrumentation. For SPURS-2, sensors included a CTD at the near-surface and another at 6 m depth, providing continuous salinity and temperature observations plus air temperature and wind measurements. Three wavegliders (https://doi.org/10.5067/SPUR2-GLID3) were deployed from the Revelle in August 2016 and again in November 2017 before final retrieval at the conclusion on the second cruise. Waveglider trajectories followed a 20x20km square loop around the moorings and a butterfly pattern around the neutrally-buoyant float. Focused around a central mooring located near 10°N,125°W, the objective of SPURS-2 (NASA-funded oceanographic process study) was to study the dynamics of the rainfall-dominated surface ocean at the western edge of the eastern Pacific fresh pool subject to high seasonal variability and strong zonal flows associated with the North Equatorial Current and Countercurrent.

2.3 Auxiliary geophysical datasets

Additional EO datasets are used to characterize the geophysical conditions at the *in situ*/satellite SSS pair measurement locations and time, and 10 days prior to the measurements, to get an estimate of the geophysical concomitant condition and history. As discussed in Boutin et al. (2016), the presence of vertical gradients in, and horizontal variability of, sea surface salinity indeed complicates comparison of satellite and *in situ* measurements. The additional EO data are used here to get a first estimates of conditions for which L-band satellite SSS measured in the first centimeters of the upper ocean within a 50-150 km diameter footprint might differ from pointwise *in situ* measurements performed in general between 10 and 5 m depth below the surface. The spatio-temporal variability of SSS within a satellite footprint (50–150 km) is a major issue for satellite SSS validation in the vicinity of river plumes, frontal zones, and significant precipitation areas, among others. Rainfall can in some cases produce vertical salinity gradients exceeding 1 pss m^{-1}; consequently, it is recommended that satellite and *in situ* SSS measurements less than 3–6 h after rain events should be considered with care when used in satellite calibration/validation analyses. To identify such situation, the Pi-MEP platform is first using CMORPH products to characterize the local value and history of rain rate and ASCAT

gridded data are used to characterize the local surface wind speed and history. For validation purpose, the ISAS monthly SSS *in situ* analysed fields at 5 m depth are collocated and compared with the satellite SSS products. The use of ISAS is motivated by the fact that it is used in the SMOS L2 official validation protocol in which systematic comparisons of SMOS L2 retrieved SSS with ISAS are done. In complement to ISAS, monthly std climatological fields from the World Ocean Atlas (WOA13) at the match-up pairs location and date are also used to have an a priori information of the local SSS variability.

2.3.1 CMORPH

Precipitation are estimated using the CMORPH 3-hourly products at $1/4°$ resolution (Joyce et al. (2004)). CMORPH (CPC MORPHing technique) produces global precipitation analyses at very high spatial and temporal resolution. This technique uses precipitation estimates that have been derived from low orbiter satellite microwave observations exclusively, and whose features are transported via spatial propagation information that is obtained entirely from geostationary satellite IR data. At present NOAA incorporate precipitation estimates derived from the passive microwaves aboard the DMSP 13, 14 and 15 (SSM/I), the NOAA-15, 16, 17 and 18 (AMSU-B), and AMSR-E and TMI aboard NASA's Aqua, TRMM and GPM spacecraft, respectively. These estimates are generated by algorithms of Ferraro (1997) for SSM/I, Ferraro et al. (2000) for AMSU-B and Kummerow et al. (2001) for TMI. Note that this technique is not a precipitation estimation algorithm but a means by which estimates from existing microwave rainfall algorithms can be combined. Therefore, this method is extremely flexible such that any precipitation estimates from any microwave satellite source can be incorporated.

With regard to spatial resolution, although the precipitation estimates are available on a grid with a spacing of 8 km (at the equator), the resolution of the individual satellite-derived estimates is coarser than that - more on the order of 12 x 15 km or so. The finer "resolution" is obtained via interpolation.

In effect, IR data are used as a means to transport the microwave-derived precipitation features during periods when microwave data are not available at a location. Propagation vector matrices are produced by computing spatial lag correlations on successive images of geostationary satellite IR which are then used to propagate the microwave derived precipitation estimates. This process governs the movement of the precipitation features only. At a given location, the shape and intensity of the precipitation features in the intervening half hour periods between microwave scans are determined by performing a time-weighting interpolation between microwave-derived features that have been propagated forward in time from the previous microwave observation and those that have been propagated backward in time from the following microwave scan. NOAA refer to this latter step as "morphing" of the features.

For the present Pi-MEP products, we only considered the 3-hourly products at 1/4 degree resolution. The entire CMORPH record (December 2002-present) for 3-hourly, 1/4 degree lat/lon resolution can be found at: `ftp://ftp.cpc.ncep.noaa.gov/precip/CMORPH_V1.0/CRT/`. CMORPH estimates cover a global belt (-180°W to 180°E) extending from 60°S to 60°N latitude and are available for the complete period of the Pi-MEP core datasets (Jan 2010-now).

2.3.2 ASCAT

Advanced SCATterometer (ASCAT) daily data produced and made available at Ifremer/CERSAT on a 0.25°x0.25° resolution grid (Bentamy and Fillon (2012)) since March 2007 are used to characterize the mean daily wind at the match-up pair location as well as the wind history during the 10-days period preceding the in situ measurement date. These wind fields are calculated based on a geostatistical method with external drift. Remotely sensed data from ASCAT are considered

as observations while those from numerical model analysis (ECMWF) are associated with the external drift. The spatial and temporal structure functions for wind speed, zonal and meridional wind components are estimated from ASCAT retrievals. Furthermore, the new procedure includes a temporal interpolation of the retrievals based on the complex empirical orthogonal function (CEOF) approach, in order to enhance the sampling length of the scatterometer observations. The resulting daily wind fields involves the main known surface wind patterns as well as some variation modes associated with temporal and spatial moving features. The accuracy of the gridded winds was investigated through comparisons with moored buoy data in Bentamy et al. (2012) and resulted in rms differences for wind speed and direction are about 1.50 m.s^{-1} and 20°.

2.3.3 ISAS

The In Situ Analysis System (ISAS), as described in Gaillard et al. (2016) is a data based re-analysis of temperature and salinity fields over the global ocean 70°N–70°S on a 1/2° grid. It was initially designed to synthesize the temperature and salinity profiles collected by the Argo program. It has been later extended to accommodate all type of vertical profile as well as time series. ISAS gridded fields are entirely based on *in situ* measurements. The methodology and configuration have been conceived to preserve as much as possible the data information content and resolution. ISAS is developed and run in a research laboratory (LOPS) in close collaboration with Coriolis, one of Argo Global Data Assembly Center and unique data provider for the Mercator operational oceanography system. In Pi-MEP, the products used are the IN-SITU_GLO_TS_OA_REP_OBSERVATIONS_013_002_b for the period 2010 to 2019 and the IN-SITU_GLO_TS_OA_NRT_OBSERVATIONS_013_002_a for the Near-Real Time (2020-2021) derived at the Coriolis data center and provided by the Copernicus Marine Environment Monitoring Service (CMEMS). The major contribution to the data set is from Argo array of profiling floats, reaching an approximate resolution of one profile every 10-days and every 3-degrees over the satellite SSS period (`http://www.umr-lops.fr/SNO-Argo/Products/ISAS-T-S-fields/`); in this version SSS from ship of opportunity thermosalinographs are not used, so that we can consider SMOS SSS validation using these measurements independent of ISAS. The ISAS optimal interpolation involves a structure function modeled as the sum of two Gaussian functions, each associated with specific time and space scales, resulting in a smoothing over typically 3 degrees. The smallest scale which can be retrieved with ISAS analysis is not smaller than 300–500 km (Kolodziejczyk et al. (2015)). For validation purpose, the ISAS monthly SSS fields at 5 m depth are collocated and compared with the satellite SSS products and included in the Pi-MEP Match-up files. In addition, the "percentage of variance" fields (PCTVAR) contained in the ISAS analyses provide information on the local variability of *in situ* SSS measurements within 1/2°x1/2° boxes.

2.3.4 World Ocean Atlas Climatology

The World Ocean Atlas 2013 version 2 (WOA13 V2) is a set of objectively analyzed (1° grid) climatological fields of *in situ* temperature, salinity and other variables provided at standard depth levels for annual, seasonal, and monthly compositing periods for the World Ocean. It also includes associated statistical fields of observed oceanographic profile data interpolated to standard depth levels on 5°, 1°, and 0.25° grids. We use these fields in complement to ISAS to characterize the climatological fields (annual mean and std) at the match-up pairs location and date.

2.4   Overview of the Match-ups generation method

The match-up production is basically a three steps process:

1. preparation of the input *in situ* and satellite data, and,

2. co-localization of satellite products with *in situ* SSS measurements.

3. co-localization of the *in situ*/satellite pair with auxiliary information.

In the following, we successively detail the approaches taken for these different steps.

2.4.1   *In situ*/Satellite data filtering

The first step consists in filtering Waveglider *in situ* data using the quality flags as described in 2.2 so that only valid salinity data remain in the final match-up files.

For high-spatial resolution *in situ* SSS measurements such as the Thermo-SalinoGraph (TSG) SSS data, as well as SSS data from surface drifters, an additional spatial filtering step is performed on the *in situ* data that will be eventually compared to the satellite SSS products. If R_{sat} is the spatial resolution of the satellite SSS product (L2 to L3-L4), the *in situ* data are spatially low pass filtered using a running median filter with a window width=R_{sat} to try to minimize the spatial representation uncertainty when comparing to the lower spatial resolution of the satellite SSS product. Both original and filtered *in situ* data are finally stored in the MDB files.

Only for satellite L2 SSS data, a third sub-step consists in filtering spurious data using the flags and associated recommendations as provided by the official data centers and described in 2.1.

2.4.2   *In situ*/Satellite Co-localization

In this step, each SSS satellite product is co-localized with the filtered *in situ* measurements. The method used for co-location is different if the satellite SSS is a swath product (so-called Level 2-types) or a time-space composite product (so-called Level 3/level 4-types).

- For L2 SSS swath data :

  If R_{sat} is the spatial resolution of the satellite swath SSS product, for each *in situ* data sample collected in the Pi-MEP database, the platform searches for all satellite SSS data found at grid nodes located within a radius of $R_{sat}/2$ from the *in situ* data location and acquired with a time-lag from the *in situ* measurement date that is less or equal than $\pm\ 12$ hours. If several satellite SSS samples are found to meet these criteria, the final satellite SSS match-up point is selected to be the closest in time from the *in situ* data measurement date. The final spatial and temporal lags between the *in situ* and satellite data are stored in the MDB files.

- For L3 and L4 composite SSS products :

  If R_{sat} is the spatial resolution of the composite satellite SSS product and D the period over which the composite product was built (e.g., periods of 1, 7, 8, 9, 10, 18 days, 1 month, etc..) with central time t_o, then for each *in situ* data sample in the Pi-MEP database within the time interval $[t_o - D/2,\ t_o + D/2]$, the platform searches for all satellite SSS data of the composite product found at grid nodes located within a radius of $R_{sat}/2$ from the *in situ* data location. If several satellite SSS product samples are found to meet these criteria, the final satellite SSS match-up point is chosen to be the composite SSS with central time t_o which is the closest in time to the *in situ* data measurement date. The final spatial and temporal lags between the *in situ* and satellite data are stored in the MDB file.

Recently, in the context of the partnership with NASA, the Pi-MEP provides a new co-localization criterion that is applied only to L2 products, called "L2-Averaged". It consists in averaging all SSS L2 swath pixels falling in a spatio-temporal window defined by R_{sat}=50km and $D = \pm 3.5$ days around the in situ location. The spatial and temporal lags stored in the MDB files correspond to the average of all lags for each in situ data.

2.4.3 MDB pair Co-localization with auxiliary data and complementary information

MDB data consist of satellite and *in situ* SSS pairs but also of auxiliary geophysical parameters such as local and history of wind speed and rain rates, as well as various information (climatology, distance to coast, mixed layer depth, barrier layer thickness, etc) that can be derived from *in situ* data and which are included in the final match-up files. The collocation of auxiliary parameters and additional information is done for each *in situ* SSS measurement contained in the match-up files as follows :

If t_{insitu} is the time/date at which the *in situ* measurement is performed, we collect:

- The ASCAT wind speed product of the same day than t_{insitu} found at the ASCAT $1/4°$ grid node with closest distance from the *in situ* data location. We then store the time series of the ASCAT wind speed at the same node for the 10 days prior to the *in situ* measurement day.

- If the *in situ* data is located within the 60°N-60°S band, we select the CMORPH 3-hourly product that is closest in time from t_{insitu} and found at the CMORPH $1/4°$ grid node with closest distance from the *in situ* data location. We then store the time series of the CMORPH rain rate at the same node for the 10 days prior to the *in situ* measurement time.

For the given month/year of the *in situ* data, we select the ISAS and WOA fields for the same month (and same year for ISAS fields) and take the SSS analysis (monthly mean, std) found at the closest grid node from the *in situ* measurement.

The distance from the *in situ* SSS data location to the nearest coast is evaluated and provided in km. We use a distance-to-coast map at $1/4°$ resolution where small islands have been removed.

When vertical profiles of salinity (S) and temperature (T) are made available from the *in situ* measurements used to build the match-up (Argo or marine mammals), the following variables are also included into each satellite/*in situ* match-up file:

1. The vertical distribution of pressure at which the profiles were measured,

2. The vertical S(z) and T(z) profiles,

3. The vertical potential density anomaly profile $\sigma_0(z)$,

4. The Mixed Layer Depth (MLD). The MLD is defined here as the depth where the potential density has increased from the reference depth (10 meter) by a threshold equivalent to $0.2°$C decrease in temperature at constant salinity: $\sigma_0 = \sigma_{010m} + \Delta\sigma_0$ with $\Delta\sigma_0 = \sigma_0(\theta_{10m} - 0.2, S_{10m}) - \sigma_0(\theta_{10m}, S_{10m})$ where θ_{10m} and S_{10m} are the temperature and salinity at the reference depth (i.e. 10 m) (de Boyer Montégut et al. (2004), de Boyer Montégut et al. (2007)).

5. The Top of the Thermocline Depth (TTD) is defined as the depth at which temperature decreases from its 10 m value by $0.2°$C.

6. The Barrier Layer thickness (BLT) is defined as the difference between the MLD and the TTD. If BLT<0, it corresponds to a vertically density compensated layer whose thickness is then the absolute value of (TTD-MLD).

7. The vertical profile of the buoyancy frequency $N^2(z)$

The resulting match-ups files are serialized as NetCDF-4 files whose structure depends on the origin of the *in situ* data and is described in section 2.4.4.

2.4.4 Content of the Match-Up NetCDF files

netcdf pimep-mdb_smap-l3-rss-v4-1m_waveglider_20100116_v01 {
dimensions:
    TIME_SAT = UNLIMITED ; // (1 currently)
    TIME_WAVEGLIDER = 2190 ;
    N_DAYS_WIND = 10 ;
    N_3H_RAIN = 80 ;
    STRING25 = 25 ;
    STRING8 = 8 ;

    variables:
float DATE_WAVEGLIDER(TIME_WAVEGLIDER) ;
    DATE_WAVEGLIDER:long_name = "Date of WAVEGLIDER" ;
    DATE_WAVEGLIDER:units = "days since 1990-01-01 00:00:00" ;
    DATE_WAVEGLIDER:standard_name = "time" ;
    DATE_WAVEGLIDER:_FillValue = -999.f ;
float LATITUDE_WAVEGLIDER(TIME_WAVEGLIDER) ;
    LATITUDE_WAVEGLIDER:long_name = "Latitude of WAVEGLIDER" ;
    LATITUDE_WAVEGLIDER:units = "degrees_north" ;
    LATITUDE_WAVEGLIDER:valid_min = -90. ;
    LATITUDE_WAVEGLIDER:valid_max = 90. ;
    LATITUDE_WAVEGLIDER:standard_name = "latitude" ;
    LATITUDE_WAVEGLIDER:_FillValue = -999.f ;
float LONGITUDE_WAVEGLIDER(TIME_WAVEGLIDER) ;
    LONGITUDE_WAVEGLIDER:long_name = "Longitude of WAVEGLIDER" ;
    LONGITUDE_WAVEGLIDER:units = "degrees_east" ;
    LONGITUDE_WAVEGLIDER:valid_min = -180. ;
    LONGITUDE_WAVEGLIDER:valid_max = 180. ;
    LONGITUDE_WAVEGLIDER:standard_name = "longitude" ;
    LONGITUDE_WAVEGLIDER:_FillValue = -999.f ;
float SSS_WAVEGLIDER(TIME_WAVEGLIDER) ;
    SSS_WAVEGLIDER:long_name = "WAVEGLIDER SSS" ;
    SSS_WAVEGLIDER:units = "1" ;
    SSS_WAVEGLIDER:salinity_scale = "Practical Salinity Scale(PSS-78)" ;
    SSS_WAVEGLIDER:standard_name = "sea_water_salinity" ;
    SSS_WAVEGLIDER:_FillValue = -999.f ;
float SST_WAVEGLIDER(TIME_WAVEGLIDER) ;
    SST_WAVEGLIDER:long_name = "WAVEGLIDER SST" ;
    SST_WAVEGLIDER:units = "degree Celsius" ;
    SST_WAVEGLIDER:standard_name = "sea_water_temperature" ;

```
        SST_WAVEGLIDER:_FillValue = -999.f ;
float SSS_WAVEGLIDER_FILTERED(TIME_WAVEGLIDER) ;
        SSS_WAVEGLIDER_FILTERED:long_name = "WAVEGLIDER SSS median filtered at
satellite spatial resolution" ;
        SSS_WAVEGLIDER_FILTERED:units = "1" ;
        SSS_WAVEGLIDER_FILTERED:salinity_scale = "Practical Salinity Scale(PSS-78)" ;
        SSS_WAVEGLIDER_FILTERED:standard_name = "sea_water_salinity" ;
        SSS_WAVEGLIDER_FILTERED:_FillValue = -999.f ;
float SST_WAVEGLIDER_FILTERED(TIME_WAVEGLIDER) ;
        SST_WAVEGLIDER_FILTERED:long_name = "WAVEGLIDER SST median filtered at
satellite spatial resolution" ;
        SST_WAVEGLIDER_FILTERED:units = "degree Celsius" ;
        SST_WAVEGLIDER_FILTERED:standard_name = "sea_water_temperature" ;
        SST_WAVEGLIDER_FILTERED:_FillValue = -999.f ;
float DISTANCE_TO_COAST_WAVEGLIDER(TIME_WAVEGLIDER) ;
        DISTANCE_TO_COAST_WAVEGLIDER:long_name = "Distance to coasts at WAVEG-
LIDER location" ;
        DISTANCE_TO_COAST_WAVEGLIDER:units = "km" ;
        DISTANCE_TO_COAST_WAVEGLIDER:_FillValue = -999.f ;
float PLATFORM_NUMBER_WAVEGLIDER(TIME_WAVEGLIDER) ;
        PLATFORM_NUMBER_WAVEGLIDER:long_name = "WAVEGLIDER unique identifier"
;
        PLATFORM_NUMBER_WAVEGLIDER:conventions = "WMO float identifier : A9IIIII" ;
        PLATFORM_NUMBER_WAVEGLIDER:units = "1" ;
        PLATFORM_NUMBER_WAVEGLIDER:_FillValue = -999.f ;
float DATE_Satellite_product(TIME_Sat) ;
        DATE_Satellite_product:long_name = "Central time of satellite SSS file" ;
        DATE_Satellite_product:units = "days since 1990-01-01 00:00:00" ;
        DATE_Satellite_product:standard_name = "time" ;
float LATITUDE_Satellite_product(TIME_WAVEGLIDER) ;
        LATITUDE_Satellite_product:long_name = "Satellite product latitude at WAVEGLIDER
location" ;
        LATITUDE_Satellite_product:units = "degrees_north" ;
        LATITUDE_Satellite_product:valid_min = -90. ;
        LATITUDE_Satellite_product:valid_max = 90. ;
        LATITUDE_Satellite_product:standard_name = "latitude" ;
        LATITUDE_Satellite_product:_FillValue = -999.f ;
float LONGITUDE_Satellite_product(TIME_WAVEGLIDER) ;
        LONGITUDE_Satellite_product:long_name = "Satellite product longitude at WAVEGLIDER
location" ;
        LONGITUDE_Satellite_product:units = "degrees_east" ;
        LONGITUDE_Satellite_product:valid_min = -180. ;
        LONGITUDE_Satellite_product:valid_max = 180. ;
        LONGITUDE_Satellite_product:standard_name = "longitude" ;
        LONGITUDE_Satellite_product:_FillValue = -999.f ;
float SSS_Satellite_product(TIME_WAVEGLIDER) ;
        SSS_Satellite_product:long_name = "Satellite product SSS at WAVEGLIDER location" ;
        SSS_Satellite_product:units = "1" ;
        SSS_Satellite_product:salinity_scale = "Practical Salinity Scale(PSS-78)" ;
```

SSS_Satellite_product:standard_name = "sea_surface_salinity" ;

SSS_Satellite_product:_FillValue = -999.f ;

float SST_Satellite_product(TIME_WAVEGLIDER) ;

SST_Satellite_product:long_name = "Satellite product SST at WAVEGLIDER location" ;

SST_Satellite_product:units = "degree Celsius" ;

SST_Satellite_product:standard_name = "sea_surface_temperature" ;

SST_Satellite_product:_FillValue = -999.f ;

float Spatial_lags(TIME_WAVEGLIDER) ;

Spatial_lags:long_name = "Spatial lag between WAVEGLIDER location and satellite SSS product pixel center" ;

Spatial_lags:units = "km" ;

Spatial_lags:_FillValue = -999.f ;

float Time_lags(TIME_WAVEGLIDER) ;

Time_lags:long_name = "Temporal lag between WAVEGLIDER time and satellite SSS product central time" ;

Time_lags:units = "days" ;

Time_lags:_FillValue = -999.f ;

float ROSSBY_RADIUS_at_WAVEGLIDER(TIME_WAVEGLIDER) ;

ROSSBY_RADIUS_at_WAVEGLIDER:long_name = "Baroclinic Rossby radius of deformation (Chelton et al., 1998) at WAVEGLIDER location" ;

ROSSBY_RADIUS_at_WAVEGLIDER:units = "km" ;

ROSSBY_RADIUS_at_WAVEGLIDER:_FillValue = -999.f ;

float Ascat_daily_wind_at_WAVEGLIDER(TIME_WAVEGLIDER) ;

Ascat_daily_wind_at_WAVEGLIDER:long_name = "Daily Ascat wind speed module at WAVEGLIDER location" ;

Ascat_daily_wind_at_WAVEGLIDER:units = "m/s" ;

Ascat_daily_wind_at_WAVEGLIDER:_FillValue = -999.f ;

float CMORPH_3h_Rain_Rate_at_WAVEGLIDER(TIME_WAVEGLIDER) ;

CMORPH_3h_Rain_Rate_at_WAVEGLIDER:long_name = "3-hourly CMORPH rain rate at WAVEGLIDER location" ;

CMORPH_3h_Rain_Rate_at_WAVEGLIDER:units = "mm/3h" ;

CMORPH_3h_Rain_Rate_at_WAVEGLIDER:_FillValue = -999.f ;

float Ascat_10_prior_days_wind_at_WAVEGLIDER(TIME_WAVEGLIDER, N_DAYS_WIND) ;

Ascat_10_prior_days_wind_at_WAVEGLIDER:long_name = "Prior 10 days time series of Ascat wind speed module at WAVEGLIDER location" ;

Ascat_10_prior_days_wind_at_WAVEGLIDER:units = "m/s" ;

Ascat_10_prior_days_wind_at_WAVEGLIDER:_FillValue = -999.f ;

float CMORPH_10_prior_days_Rain_Rate_at_WAVEGLIDER(TIME_WAVEGLIDER, N_3H_RAIN) ;

CMORPH_10_prior_days_Rain_Rate_at_WAVEGLIDER:long_name = "Prior 10 days times series of 3-hourly CMORPH Rain Rate at WAVEGLIDER location" ;

CMORPH_10_prior_days_Rain_Rate_at_WAVEGLIDER:units = "mm/3h" ;

CMORPH_10_prior_days_Rain_Rate_at_WAVEGLIDER:_FillValue = -999.f ;

float SSS_ISAS_at_WAVEGLIDER(TIME_WAVEGLIDER) ;

SSS_ISAS_at_WAVEGLIDER:long_name = "ISAS SSS (5m depth) at WAVEGLIDER location" ;

SSS_ISAS_at_WAVEGLIDER:units = "1" ;

SSS_ISAS_at_WAVEGLIDER:salinity_scale = "Practical Salinity Scale(PSS-78)" ;

SSS_ISAS_at_WAVEGLIDER:standard_name = "sea_water_salinity" ;

SSS_ISAS_at_WAVEGLIDER:_FillValue = -999.f ;
float SSS_PCTVAR_ISAS_at_WAVEGLIDER(TIME_WAVEGLIDER) ;
    SSS_PCTVAR_ISAS_at_WAVEGLIDER:long_name = "Error on ISAS SSS (5m depth) at
WAVEGLIDER location (% variance)" ;
    SSS_PCTVAR_ISAS_at_WAVEGLIDER:units = "%" ;
    SSS_PCTVAR_ISAS_at_WAVEGLIDER:_FillValue = -999.f ;
float SSS_WOA13_at_WAVEGLIDER(TIME_WAVEGLIDER) ;
    SSS_WOA13_at_WAVEGLIDER:long_name = "WOA 2013 (DECAV-1deg) SSS (0m depth)
at WAVEGLIDER location" ;
    SSS_WOA13_at_WAVEGLIDER:units = "1" ;
    SSS_WOA13_at_WAVEGLIDER:salinity_scale = "Practical Salinity Scale(PSS-78)" ;
    SSS_WOA13_at_WAVEGLIDER:standard_name = "sea_surface_salinity" ;
    SSS_WOA13_at_WAVEGLIDER:_FillValue = -999.f ;
float SSS_STD_WOA13_at_WAVEGLIDER(TIME_WAVEGLIDER) ;
    SSS_STD_WOA13_at_WAVEGLIDER:long_name = "WOA 2013 (DECAV-1deg) SSS STD
(0m depth) at WAVEGLIDER location " ;
    SSS_STD_WOA13_at_WAVEGLIDER:units = "1" ;
    SSS_STD_WOA13_at_WAVEGLIDER:_FillValue = -999.f ;
float SSS_ISAS15_at_WAVEGLIDER(N_prof) ;
    SSS_ISAS15_at_WAVEGLIDER:long_name = "Monthly ISAS-15 SSS (5m depth) at WAVEG-
LIDER location" ;
    SSS_ISAS15_at_WAVEGLIDER:units = "1" ;
    SSS_ISAS15_at_WAVEGLIDER:salinity_scale = "Practical Salinity Scale (PSS-78)" ;
    SSS_ISAS15_at_WAVEGLIDER:standard_name = "sea_water_salinity" ;
    SSS_ISAS15_at_WAVEGLIDER:_FillValue = -999.f ;
float SSS_PCTVAR_ISAS15_at_WAVEGLIDER(N_prof) ;
    SSS_PCTVAR_ISAS15_at_WAVEGLIDER:long_name = "Error on monthly ISAS-15 SSS
(5m depth) at WAVEGLIDER location (% variance)" ;
    SSS_PCTVAR_ISAS15_at_WAVEGLIDER:units = "%" ;
    SSS_PCTVAR_ISAS15_at_WAVEGLIDER:_FillValue = -999.f ;
float SSS_WOA18_at_WAVEGLIDER(N_prof) ;
    SSS_WOA18_at_WAVEGLIDER:long_name = "Monthly WOA 2018 (DECAV-1deg) SSS
(0m depth) at WAVEGLIDER location" ;
    SSS_WOA18_at_WAVEGLIDER:units = "1" ;
    SSS_WOA18_at_WAVEGLIDER:salinity_scale = "Practical Salinity Scale (PSS-78)" ;
    SSS_WOA18_at_WAVEGLIDER:standard_name = "sea_surface_salinity" ;
    SSS_WOA18_at_WAVEGLIDER:_FillValue = -999.f ;
float SSS_STD_WOA18_at_WAVEGLIDER(N_prof) ;
    SSS_STD_WOA18_at_WAVEGLIDER:long_name = "Monthly WOA 2018 (DECAV-1deg)
SSS STD (0m depth) at WAVEGLIDER location " ;
    SSS_STD_WOA18_at_WAVEGLIDER:units = "1" ;
    SSS_STD_WOA18_at_WAVEGLIDER:_FillValue = -999.f ;
float SEA_ICE_CONCENTRATION_at_WAVEGLIDER(N_prof) ;
    SEA_ICE_CONCENTRATION_at_WAVEGLIDER:long_name = "Daily sea ice area frac-
tion (EUMETSAT OSI-SAF OSI-450) at WAVEGLIDER location (%)" ;
    SEA_ICE_CONCENTRATION_at_WAVEGLIDER:units = "1" ;
    SEA_ICE_CONCENTRATION_at_WAVEGLIDER:standard_name = "sea_ice_area_fraction"
;
    SEA_ICE_CONCENTRATION_at_WAVEGLIDER:_FillValue = -999.f ;

float CCMP_6h_Wind_Speed_at_WAVEGLIDER(N_prof) ;
        CCMP_6h_Wind_Speed_at_WAVEGLIDER:long_name = "6-hourly CCMP wind speed at
WAVEGLIDER location" ;
        CCMP_6h_Wind_Speed_at_WAVEGLIDER:units = "m s-1" ;
        CCMP_6h_Wind_Speed_at_WAVEGLIDER:standard_name = "wind_speed" ;
        CCMP_6h_Wind_Speed_at_WAVEGLIDER:_FillValue = -999.f ;
float CCMP_10_prior_days_Wind_Speed_at_WAVEGLIDER(N_prof, N_DAYS_WIND_CCMP) ;
        CCMP_10_prior_days_Wind_Speed_at_WAVEGLIDER:long_name = "Prior 10 days time se-
ries of CCMP wind speed at WAVEGLIDER location" ;
        CCMP_10_prior_days_Wind_Speed_at_WAVEGLIDER:units = "m s-1" ;
        CCMP_10_prior_days_Wind_Speed_at_WAVEGLIDER:standard_name = "wind_speed" ;
        CCMP_10_prior_days_Wind_Speed_at_WAVEGLIDER:_FillValue = -999.f ;
float CDM_GLOBCOLOUR_at_WAVEGLIDER(N_prof) ;
        CDM_GLOBCOLOUR_at_WAVEGLIDER:long_name = "8-day Coloured dissolved and de-
trital organic materials - mean of the binned pixels at WAVEGLIDER location" ;
        CDM_GLOBCOLOUR_at_WAVEGLIDER:units = "m-1" ;
        CDM_GLOBCOLOUR_at_WAVEGLIDER:standard_name = "volume_absorption_coefficient_of_radiative_flux_in_
;
        CDM_GLOBCOLOUR_at_WAVEGLIDER:_FillValue = -999.f ;
float CHL1_GLOBCOLOUR_at_WAVEGLIDER(N_prof) ;
        CHL1_GLOBCOLOUR_at_WAVEGLIDER:long_name = "8-day Chlorophyll concentration
- mean of the binned pixels at WAVEGLIDER location" ;
        CHL1_GLOBCOLOUR_at_WAVEGLIDER:units = "mg m-3" ;
        CHL1_GLOBCOLOUR_at_WAVEGLIDER:standard_name = "mass_concentration_of_chlorophyll_a_in_sea_water
;
        CHL1_GLOBCOLOUR_at_WAVEGLIDER:_FillValue = -999.f ;
float EVAPORATION_OAFLUX_at_WAVEGLIDER(N_prof) ;
        EVAPORATION_OAFLUX_at_WAVEGLIDER:long_name = "Daily mean evaporation rate
(OAFlux) at WAVEGLIDER location" ;
        EVAPORATION_OAFLUX_at_WAVEGLIDER:units = "cm year-1" ;
        EVAPORATION_OAFLUX_at_WAVEGLIDER:_FillValue = -999.f ;
float SSS_SCRIPPS_at_WAVEGLIDER(N_prof) ;
        SSS_SCRIPPS_at_WAVEGLIDER:long_name = "Argo gridded monthly mean SSS (0m
depth) from SCRIPPS (Roemmich-Gilson) at WAVEGLIDER location" ;
        SSS_SCRIPPS_at_WAVEGLIDER:units = "1" ;
        SSS_SCRIPPS_at_WAVEGLIDER:salinity_scale = "Practical Salinity Scale (PSS-78)" ;
        SSS_SCRIPPS_at_WAVEGLIDER:standard_name = "sea_water_salinity" ;
        SSS_SCRIPPS_at_WAVEGLIDER:_FillValue = -999.f ;
float SSS_IPRC_at_WAVEGLIDER(N_prof) ;
        SSS_IPRC_at_WAVEGLIDER:long_name = "Argo gridded monthly mean SSS (0m depth)
from IPRC at WAVEGLIDER location" ;
        SSS_IPRC_at_WAVEGLIDER:units = "1" ;
        SSS_IPRC_at_WAVEGLIDER:salinity_scale = "Practical Salinity Scale (PSS-78)" ;
        SSS_IPRC_at_WAVEGLIDER:standard_name = "sea_water_salinity" ;
        SSS_IPRC_at_WAVEGLIDER:_FillValue = -999.f ;
float SST_AVHRR_at_WAVEGLIDER(N_prof) ;
        SST_AVHRR_at_WAVEGLIDER:long_name = "Daily OI AVHRR-only v2 SST (Reynolds
et al., 2007) at WAVEGLIDER location" ;
        SST_AVHRR_at_WAVEGLIDER:units = "degree Celsius" ;

SST_AVHRR_at_WAVEGLIDER:standard_name = "sea_water_temperature" ;
SST_AVHRR_at_WAVEGLIDER:_FillValue = -999.f ;
float U_EKMAN_GLOBCURRENT_at_WAVEGLIDER(N_prof) ;
U_EKMAN_GLOBCURRENT_at_WAVEGLIDER:long_name = "15m depth Ekman current velocity: zonal component at WAVEGLIDER location" ;
U_EKMAN_GLOBCURRENT_at_WAVEGLIDER:units = "m s-1" ;
U_EKMAN_GLOBCURRENT_at_WAVEGLIDER:_FillValue = -999.f ;
float V_EKMAN_GLOBCURRENT_at_WAVEGLIDER(N_prof) ;
V_EKMAN_GLOBCURRENT_at_WAVEGLIDER:long_name = "15m depth Ekman current velocity: meridian component at WAVEGLIDER location" ;
V_EKMAN_GLOBCURRENT_at_WAVEGLIDER:units = "m s-1" ;
V_EKMAN_GLOBCURRENT_at_WAVEGLIDER:_FillValue = -999.f ;
float U_GEOSTROPHIC_GLOBCURRENT_at_WAVEGLIDER(N_prof) ;
U_GEOSTROPHIC_GLOBCURRENT_at_WAVEGLIDER:long_name = "Absolute geostrophic velocity: zonal component at WAVEGLIDER location" ;
U_GEOSTROPHIC_GLOBCURRENT_at_WAVEGLIDER:units = "m s-1" ;
U_GEOSTROPHIC_GLOBCURRENT_at_WAVEGLIDER:_FillValue = -999.f ;
float V_GEOSTROPHIC_GLOBCURRENT_at_WAVEGLIDER(N_prof) ;
V_GEOSTROPHIC_GLOBCURRENT_at_WAVEGLIDER:long_name = "Absolute geostrophic velocity: meridian component at WAVEGLIDER location" ;
V_GEOSTROPHIC_GLOBCURRENT_at_WAVEGLIDER:units = "m s-1" ;
V_GEOSTROPHIC_GLOBCURRENT_at_WAVEGLIDER:_FillValue = -999.f ;

// global attributes:
:Conventions = "CF-1.6" ;
:title = "Waveglider Match-Up Database" ;
:Satellite_product_name = "SMAP SSS L3 v4 - Monthly (RSS)" ;
:Satellite_product_spatial_resolution = "70 km" ;
:Satellite_product_temporal_resolution = "Monthly" ;
:Satellite_product_filename = " v4/monthly/2015/RSS_smap_SSS_L3_monthly_2015_04_FNL_v04.0.nc" ;
:Match-Up_spatial_window_radius_in_km = 35;
:Match-Up_temporal_window_radius_in_days = 15;
:start_time = "20100114T000005Z" ;
:stop_time = "20100118T235026Z" ;
:northernmost_latitude = 77.676f ;
:sourthenmost_latitude = -66.423f ;
:westernmost_longitude = -179.219f ;
:easternmost_longitude = 179.199f ;
:geospatial_lat_units = "degrees north" ;
:geospatial_lat_resolution = "70 km" ;
:geospatial_lon_units = "degrees east" ;
:geospatial_lon_resolution = "70 km" ;
:institution = "ESA-IFREMER-ODL-OCEANSCOPE" ;
:project_name = "SMOS Pilot-Mission Exploitation Platform (Pi-MEP) for salinity" ;
:project_url = "https://www.salinity-pimep.org" ;
:license = "Pi-MEP data use is free and open" ;
:product_version = "1.0" ;
:keywords = "Oceans > Ocean Salinity > Sea Surface Salinity" ;
:acknowledgment = "Please acknowledge the use of these data with the following state-

ment: These data were provided by the SMOS Pilot-Mission Exploitation Platform (Pi-MEP) for salinity" ;

    :source = " _{v4/monthly/2015/RSS_smap_SSS_L3_monthly_2015_04_FNL_v04.0.nc} " ;

    :references = "https://www.salinity-pimep.org" ;

    :history = "Processed on 2018-04-18 using MDB_generator" ;

    :date_created = "2018-04-18 17:09:30" ;

}

2.5 MDB characteristics for each specific *in situ*/satellite pair

2.5.1 Number of paired SSS data as a function of time and distance to coast

Figure 1 shows the time (a) and distance to coast (b) distributions of the match-ups between Waveglider and SMAP SSS L3 v4 - Monthly (RSS) for the SPURS 2 Pi-MEP region and for the full satellite product period.
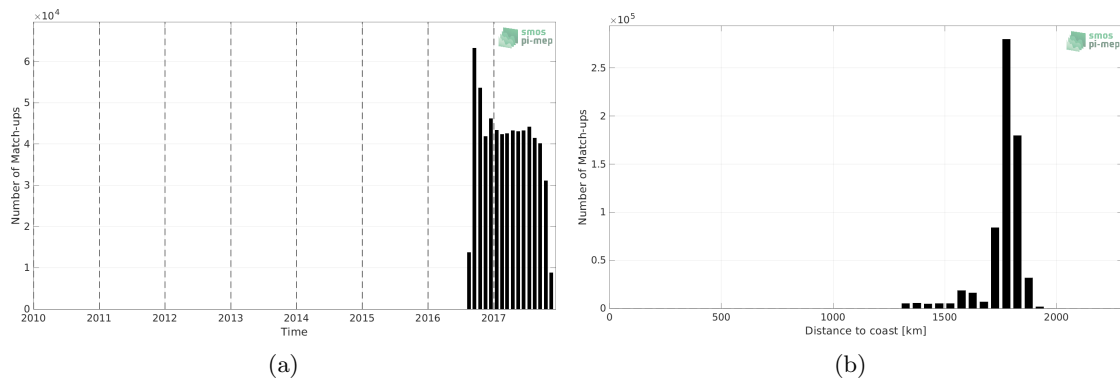
Figure 1: Number of match-ups between Waveglider and SMAP SSS L3 v4 - Monthly (RSS) SSS as a function of time (a) and as function of the distance to coast (b) over the SPURS 2 Pi-MEP region and for the full satellite product period.

2.5.2 Histograms of the SSS match-ups

Figure 2 shows the SSS distribution of Waveglider (a) and SMAP SSS L3 v4 - Monthly (RSS) (b) considering all match-up pairs per bins of 0.1 over the SPURS 2 Pi-MEP region and for the full satellite product period.

(a)   (b)
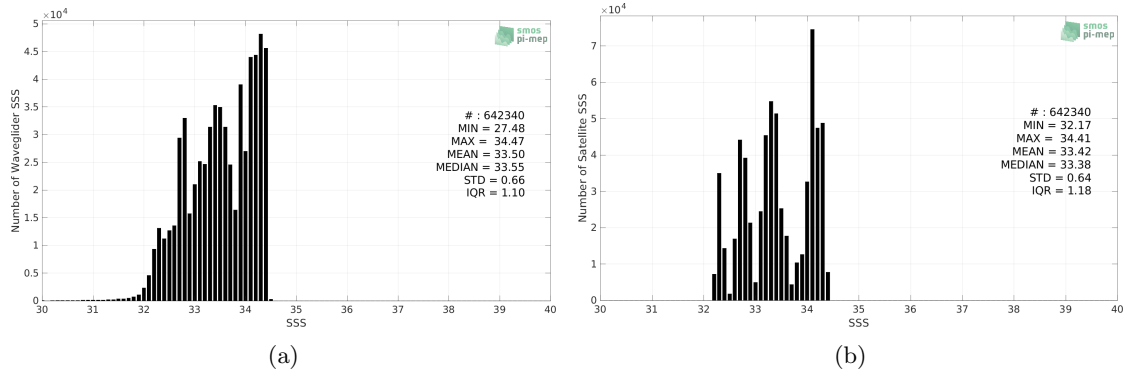
Figure 2: Histograms of SSS from Waveglider (a) and SMAP SSS L3 v4 - Monthly (RSS) (b) considering all match-up pairs per bins of 0.1 over the SPURS 2 Pi-MEP region and for the full satellite product period.

2.5.3 Spatial Distribution of Match-ups

The number of SSS match-ups between Waveglider SSS and the SMAP SSS L3 v4 - Monthly (RSS) SSS product for the SPURS 2 Pi-MEP region over 1°×1° boxes and for the full satellite product period is shown in Figure 3.
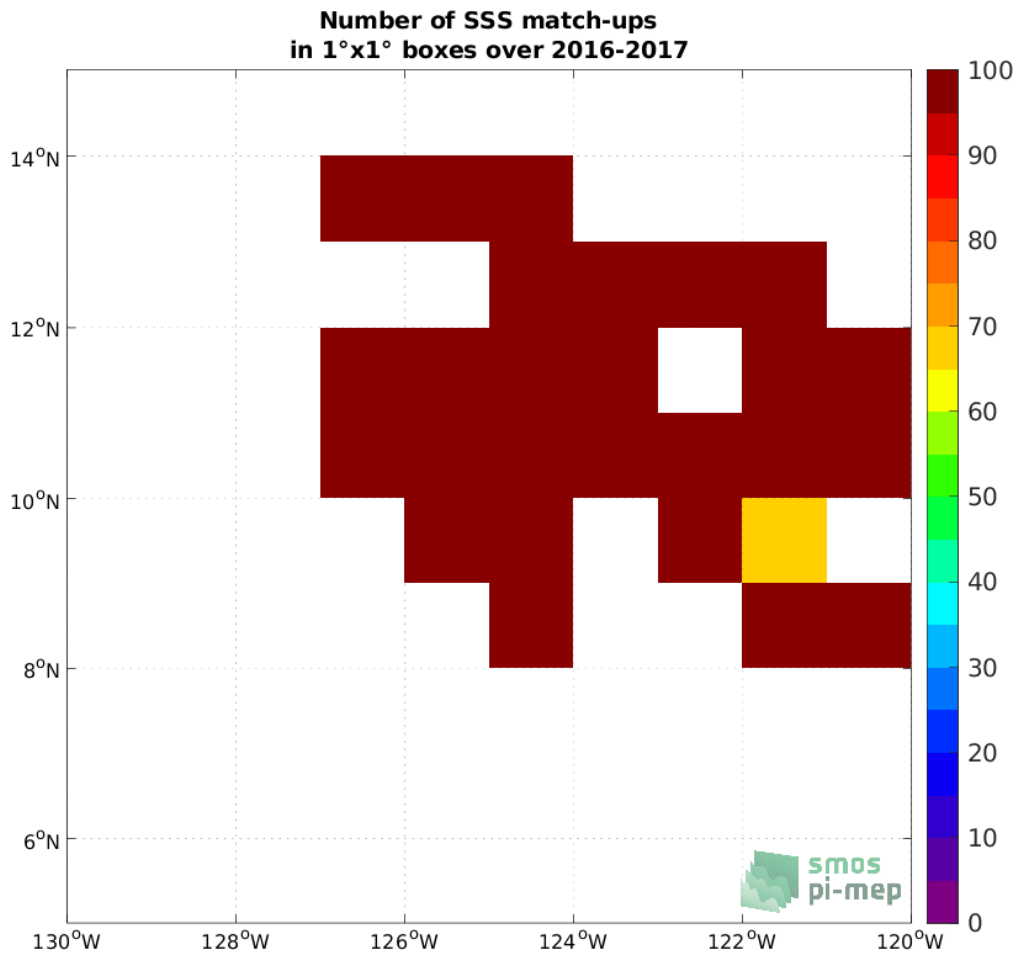
Figure 3: Number of SSS match-ups between Waveglider SSS and the SMAP SSS L3 v4 - Monthly (RSS) SSS product for the SPURS 2 Pi-MEP region over 1°×1° boxes and for the full satellite product period.

2.5.4 Histograms of the spatial and temporal lags of the match-ups pairs

Figure 4 reveals the spatial (left) and temporal (right) lags between the location/time of the Waveglider measurement and the position/date of the corresponding SMAP SSS L3 v4 - Monthly (RSS) SSS pixel of all match-ups pairs.
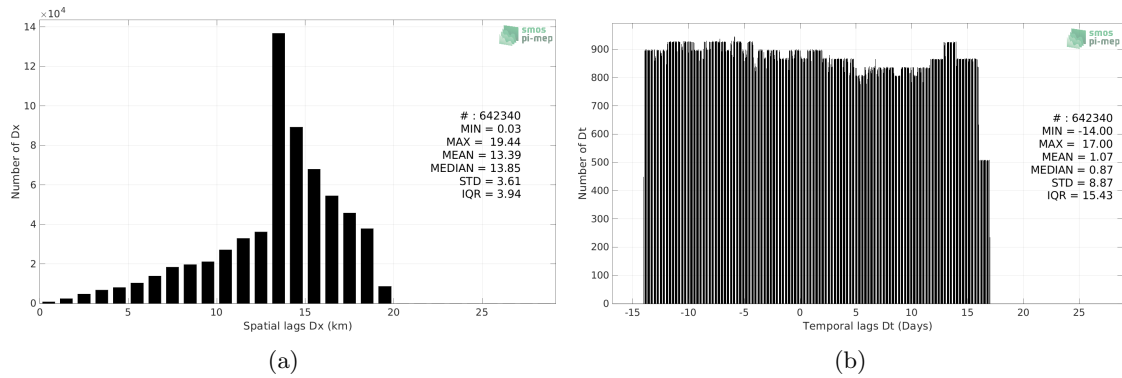
Figure 4: Histograms of the spatial (a) and temporal (b) lags between the location/time of the Waveglider measurement and the date of the corresponding SMAP SSS L3 v4 - Monthly (RSS) SSS pixel.

3 MDB file Analyses

3.1 Spatial Maps of the Temporal mean and Std of *in situ* and satellite SSS and of their difference (ΔSSS)

In Figure 5, we show maps of temporal mean (left) and standard deviation (right) of the SMAP SSS L3 v4 - Monthly (RSS) (top) and of the Waveglider *in situ* dataset at the collected Pi-MEP match-up pairs. The temporal mean and std are gridded over the full satellite product period and over spatial boxes of size 1°×1°.

At the bottom of Figure 5, the temporal mean (left) and standard deviation (right) of the differences between the satellite SSS product and *in situ* data found at match-up pairs, namely ΔSSS(Satellite -Waveglider), is also gridded over the full satellite product period and over spatial boxes of size 1°×1°.

(a) MEAN(Satellite SSS)

(b) Std(Satellite SSS)

(c) MEAN(Waveglider SSS)

(d) Std(Waveglider SSS)

(e) MEAN(ΔSSS) (Satellite - Waveglider)

(f) Std(ΔSSS) (Satellite - Waveglider)
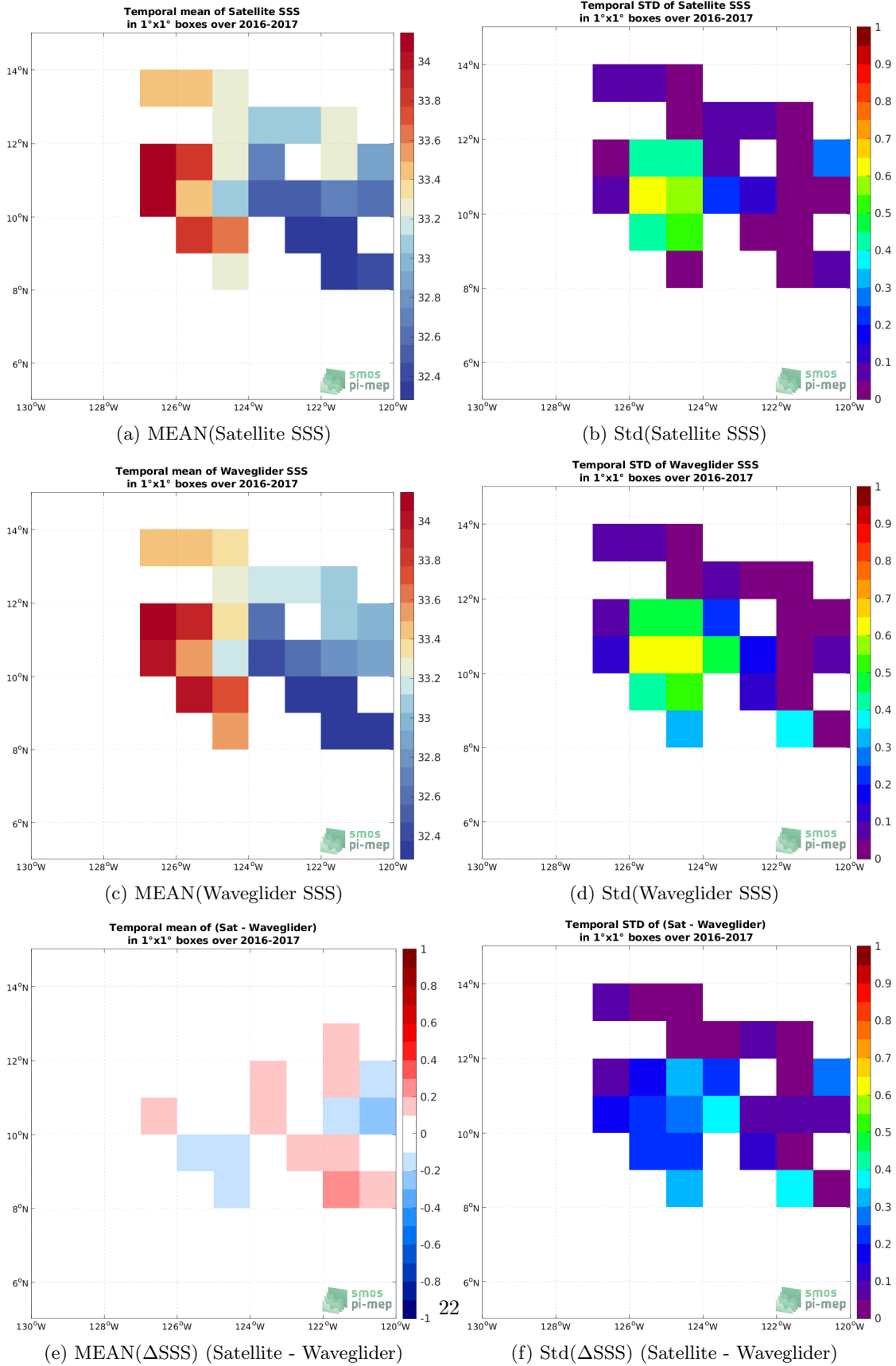
Figure 5: Temporal mean (left) and Std (right) of SSS from SMAP SSS L3 v4 - Monthly (RSS) (top), Waveglider (middle), and of ΔSSS (Satellite - Waveglider). Only match-up pairs are used to generate these maps.

3.2 Time series of the monthly median and Std of *in situ* and satellite SSS and of their difference (ΔSSS)

In the top panel of Figure 6, we show the time series of the monthly median SSS estimated over the full SPURS 2 Pi-MEP region for both SMAP SSS L3 v4 - Monthly (RSS) satellite SSS product (in black) and the Waveglider *in situ* dataset (in blue) at the collected Pi-MEP match-up pairs.

In the middle panel of Figure 6, we show the time series of the monthly median of ΔSSS (Satellite - Waveglider) for the collected Pi-MEP match-up pairs and estimated over the full SPURS 2 Pi-MEP region.

In the bottom panel of Figure 6, we show the time series of the monthly standard deviation of ΔSSS (Satellite - Waveglider) for the collected Pi-MEP match-up pairs and estimated over the full SPURS 2 Pi-MEP region.
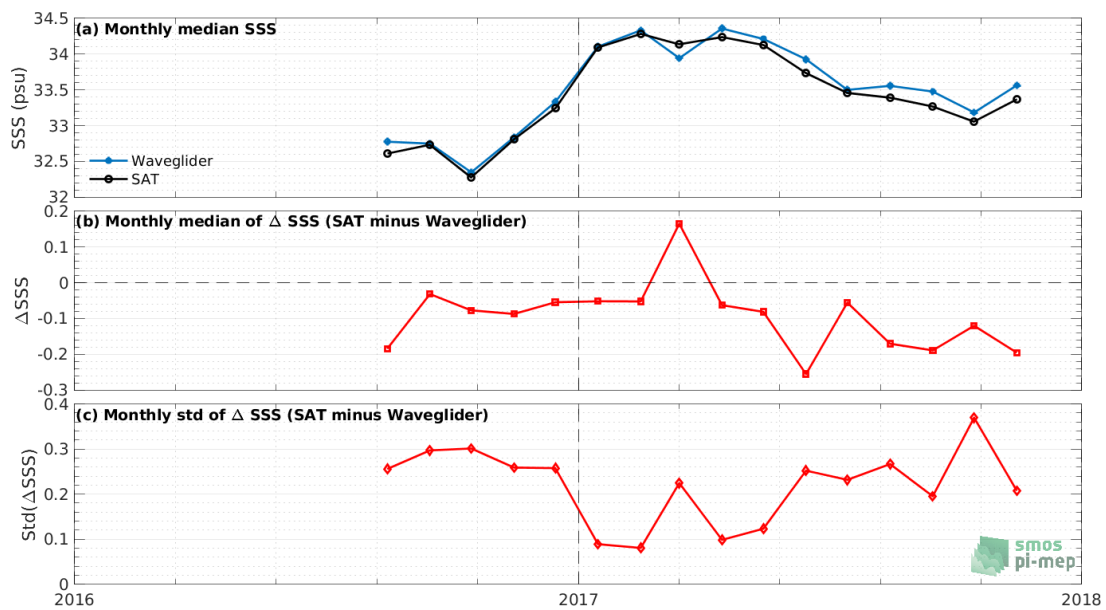
Figure 6: Time series of the monthly median SSS (top), median of ΔSSS (Satellite - Waveglider) and Std of ΔSSS (Satellite - Waveglider) over the SPURS 2 Pi-MEP region considering all match-ups collected by the Pi-MEP.

3.3 Zonal mean and Std of *in situ* and satellite SSS and of the difference (ΔSSS)

In Figure 7 left panel, we show the zonal mean SSS considering all Pi-MEP match-up pairs for both SMAP SSS L3 v4 - Monthly (RSS) satellite SSS product (in black) and the Waveglider *in situ* dataset (in blue). The full satellite SSS product period is used to derive the mean.

In the right panel of Figure 7, we show the zonal mean of ΔSSS (Satellite - Waveglider) for all the collected Pi-MEP match-up pairs estimated over the full satellite product period.
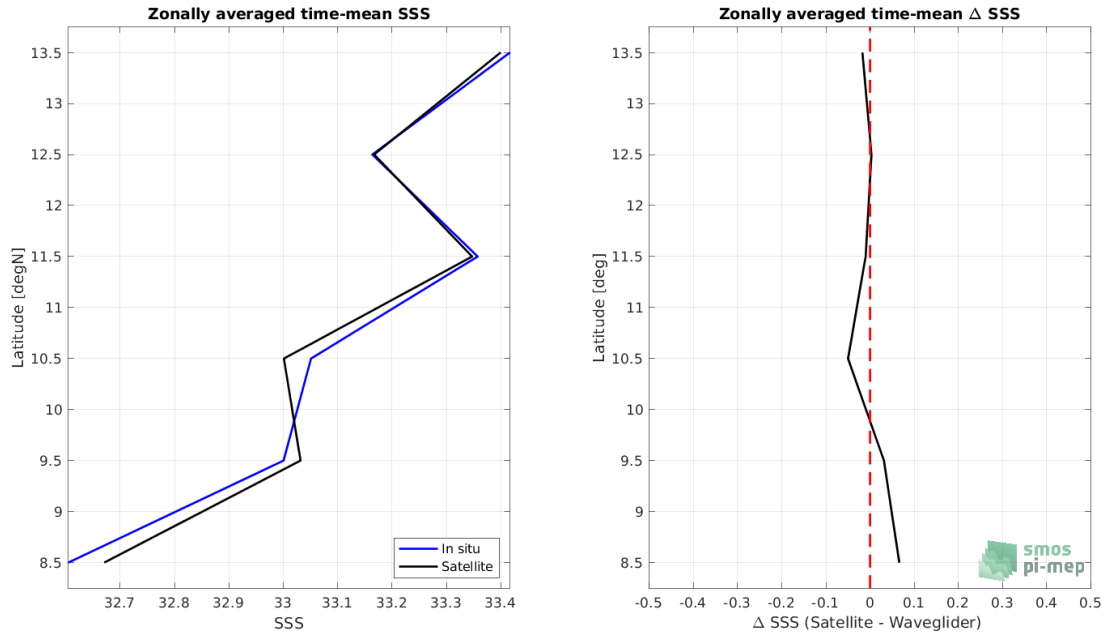
Figure 7: Left panel: Zonal mean SSS from SMAP SSS L3 v4 - Monthly (RSS) satellite product (black) and from Waveglider (blue). Right panel: Zonal mean of ΔSSS (Satellite - Waveglider) for all the collected Pi-MEP match-up pairs estimated over the full satellite product period.

3.4 Scatterplots of satellite vs *in situ* SSS by latitudinal bands

In Figure 8, contour maps of the concentration of SMAP SSS L3 v4 - Monthly (RSS) SSS (y-axis) versus Waveglider SSS (x-axis) at match-up pairs for different latitude bands: (a) 80°S-80°N, (b) 20°S-20°N, (c) 40°S-20°S and 20°N-40°N and (d) 60°S-40°S and 40°N-60°N. For each plot, the red line shows x=y. The black thin and dashed lines indicate a linear fit through the data cloud and the ±95% confidence levels, respectively. The number match-up pairs n, the slope and R^2 coefficient of the linear fit, the root mean square (RMS) and the mean bias between satellite and *in situ* data are indicated for each latitude band in each plots.

(a) $0° \leq |\text{LAT}| \leq 80°$

(b) $0° \leq |\text{LAT}| \leq 20°$

(c) $20° \leq |\text{LAT}| \leq 40°$

(d) $40° \leq |\text{LAT}| \leq 60°$
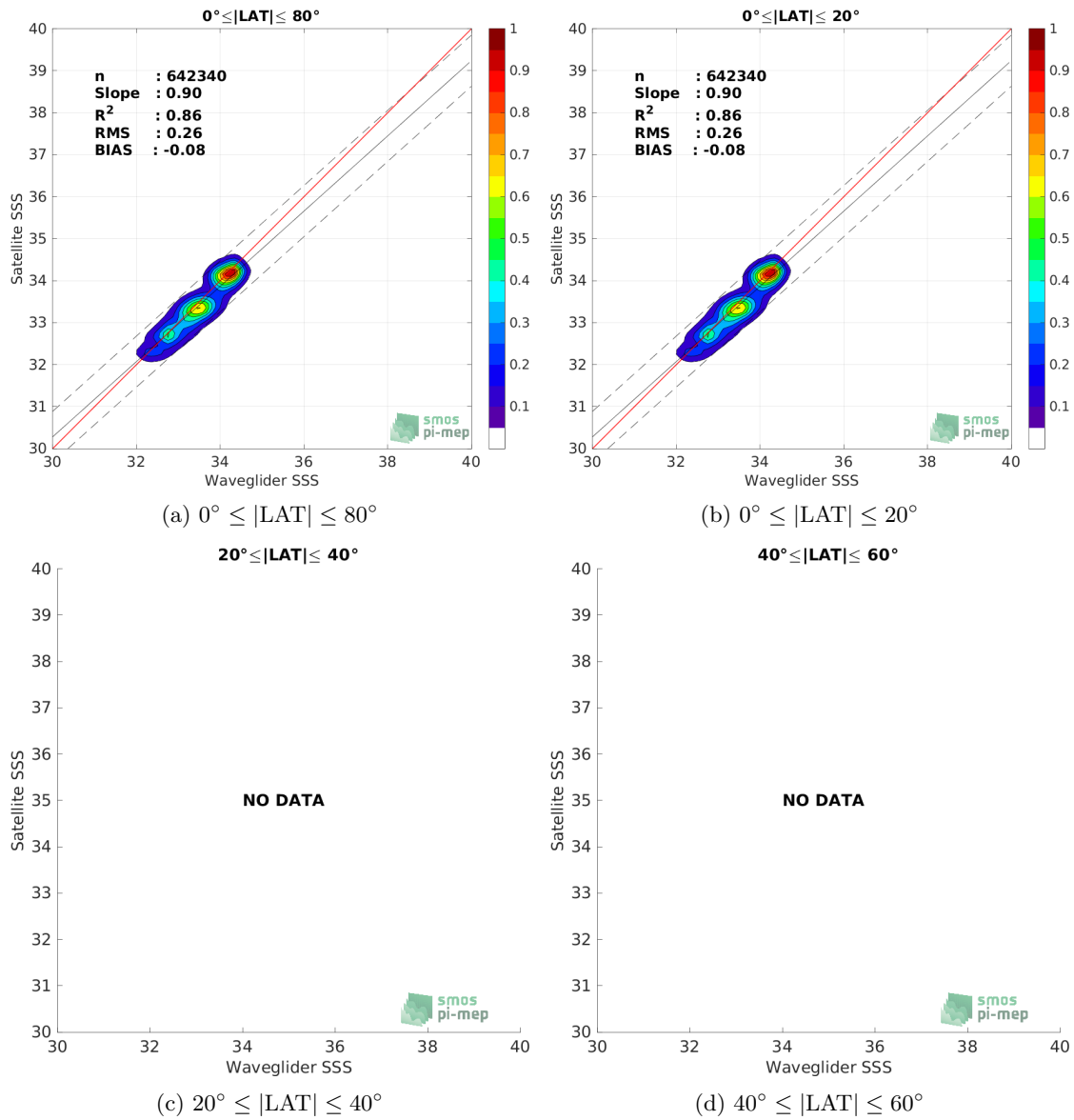
Figure 8: Contour maps of the concentration of SMAP SSS L3 v4 - Monthly (RSS) SSS (y-axis) versus Waveglider SSS (x-axis) at match-up pairs for different latitude bands. For each plot, the red line shows x=y. The black thin and dashed lines indicate a linear fit through the data cloud and the ±95% confidence levels, respectively. The number match-up pairs n, the slope and R^2 coefficient of the linear fit, the root mean square (RMS) and the mean bias between satellite and *in situ* data are indicated for each latitude band in each plots.

3.5 Time series of the monthly median and Std of ΔSSS sorted by latitudinal bands

In Figure 9, time series of the monthly median (red curves) of ΔSSS (Satellite - Waveglider) and ±1 Std (black vertical thick bars) as function of time for all the collected Pi-MEP match-up

25

pairs estimated over the SPURS 2 Pi-MEP region and for the full satellite product period are shown for different latitude bands: (a) 80°S-80°N, (b) 20°S-20°N, (c) 40°S-20°S and 20°N-40°N and (d) 60°S-40°S and 40°N-60°N.

(a) $0° \leq |LAT| \leq 80°$

(b) $0° \leq |LAT| \leq 20°$

(c) $20° \leq |LAT| \leq 40°$

(d) $40° \leq |LAT| \leq 60°$
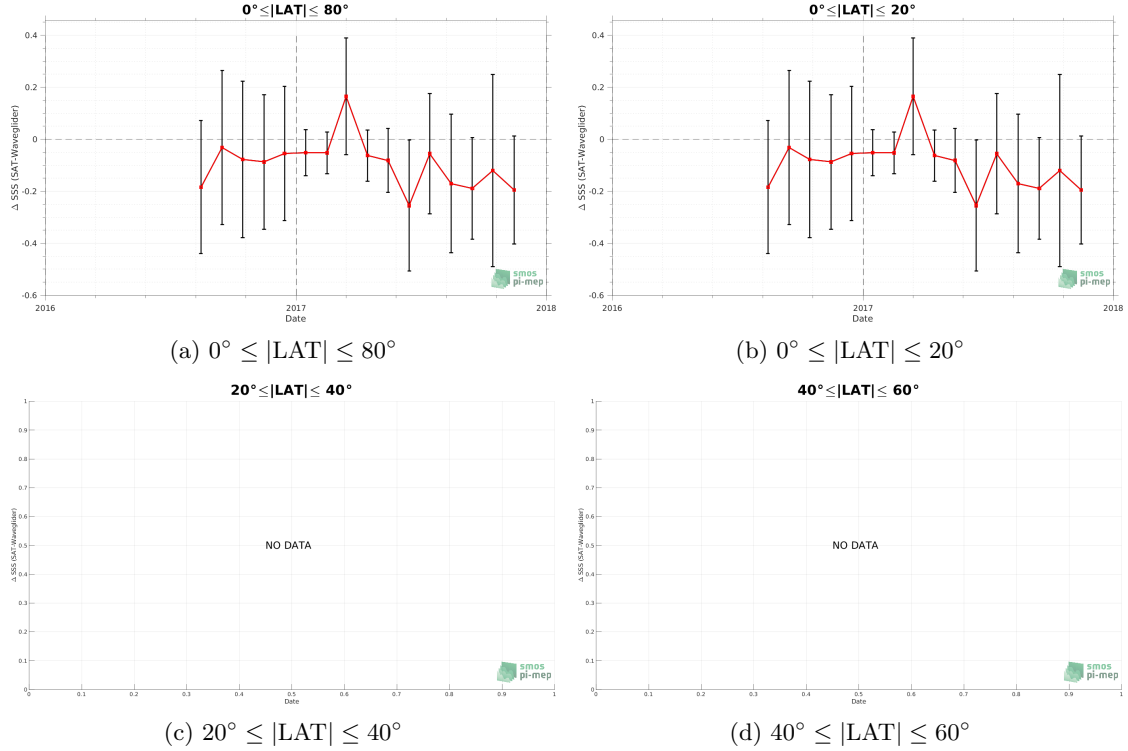
Figure 9: Monthly median (red curves) of ΔSSS (Satellite - Waveglider) and ±1 Std (black vertical thick bars) as function of time for all the collected Pi-MEP match-up pairs estimated over the SPURS 2 Pi-MEP region and for the full satellite product period are shown for different latitude bands: (a) 80°S-80°N, (b) 20°S-20°N, (c) 40°S-20°S and 20°N-40°N and (d) 60°S-40°S and 40°N-60°N.

3.6 ΔSSS sorted as function of geophysical parameters

In Figure 10, we classify the match-up differences ΔSSS (Satellite - *in situ*) between SMAP SSS L3 v4 - Monthly (RSS) and Waveglider SSS as function of the geophysical conditions at match-up points. The median and std of ΔSSS (Satellite - Waveglider) is thus evaluated as function of the

- *in situ* SSS values per bins of width 0.2,

- *in situ* SST values per bins of width 1°C,

- ASCAT daily wind values per bins of width 1 m/s,

- CMORPH 3-hourly rain rates per bins of width 1 mm/h,

- distance to coasts per bins of width 50 km,

- *in situ* measurement depth (if relevant).

26

(a) Waveglider SSS

(b) Waveglider SST

(c) ASCAT Wind Speed

(d) CMORPH Rain rate

(e) Distance to coast
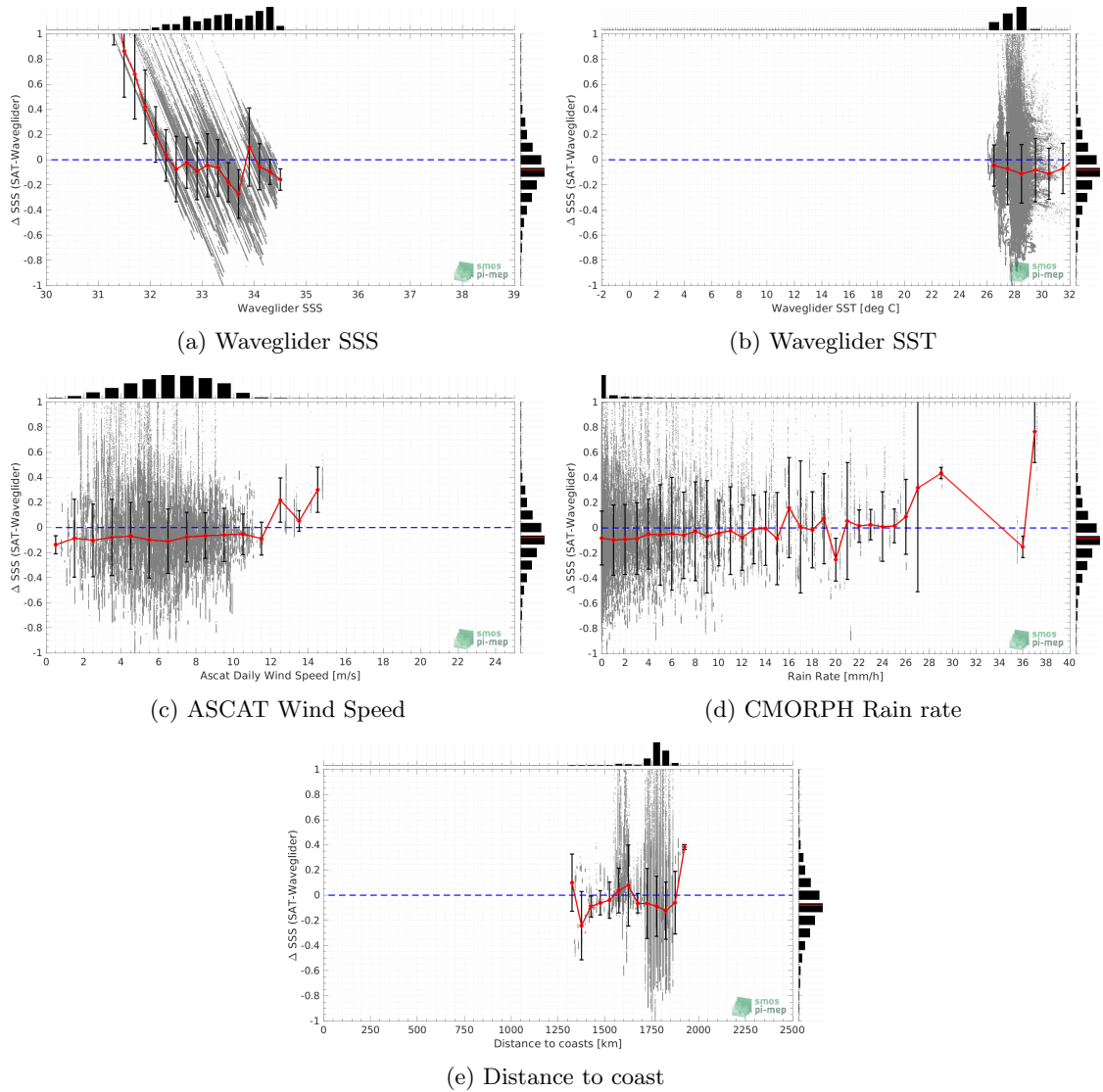
Figure 10: ΔSSS (Satellite - Waveglider) sorted as function of Waveglider SSS values a), Waveglider SST b), ASCAT Wind speed c), CMORPH rain rate d) and distance to coast (e). In all plots the median and Std of ΔSSS for each bin is indicated by the red curves and black vertical thick bars (±1 Std)

3.7 ΔSSS maps and statistics for different geophysical conditions

In Figures 11 and 12, we focus on sub-datasets of the match-up differences ΔSSS (Satellite - *in situ*) between SMAP SSS L3 v4 - Monthly (RSS) and Waveglider for the following specific geophysical conditions:

- **C1**:if the local value at *in situ* location of estimated rain rate is zero, mean daily wind is in the range [3, 12] m/s, the SST is > 5°C and distance to coast is > 800 km.

- **C2**:if the local value at *in situ* location of estimated rain rate is zero, mean daily wind is

in the range [3, 12] m/s.

- **C3**:if the local value at *in situ* location of estimated rain rate is high (ie. > 1 mm/h) and mean daily wind is low (ie. < 4 m/s).

- **C5**:if the *in situ* data is located where the climatological SSS standard deviation is low (ie. above < 0.2).

- **C6**:if the *in situ* data is located where the climatological SSS standard deviation is high (ie. above > 0.2).

For each of these conditions, the temporal mean (gridded over spatial boxes of size $1° \times 1°$) and the histogram of the difference ΔSSS (Satellite - *in situ*) are presented.

(a) RR=0 mm/h, 3< U_{10} <12 m/s, SST>5°C, distance to coast > 800 km

(b) RR=0 mm/h, 3< U_{10} <12 m/s

(c) RR>1mm/h and U_{10} <4m/s

(d) WOA2013 SSS Std<0.2

(e) WOA2013 SSS Std>0.2
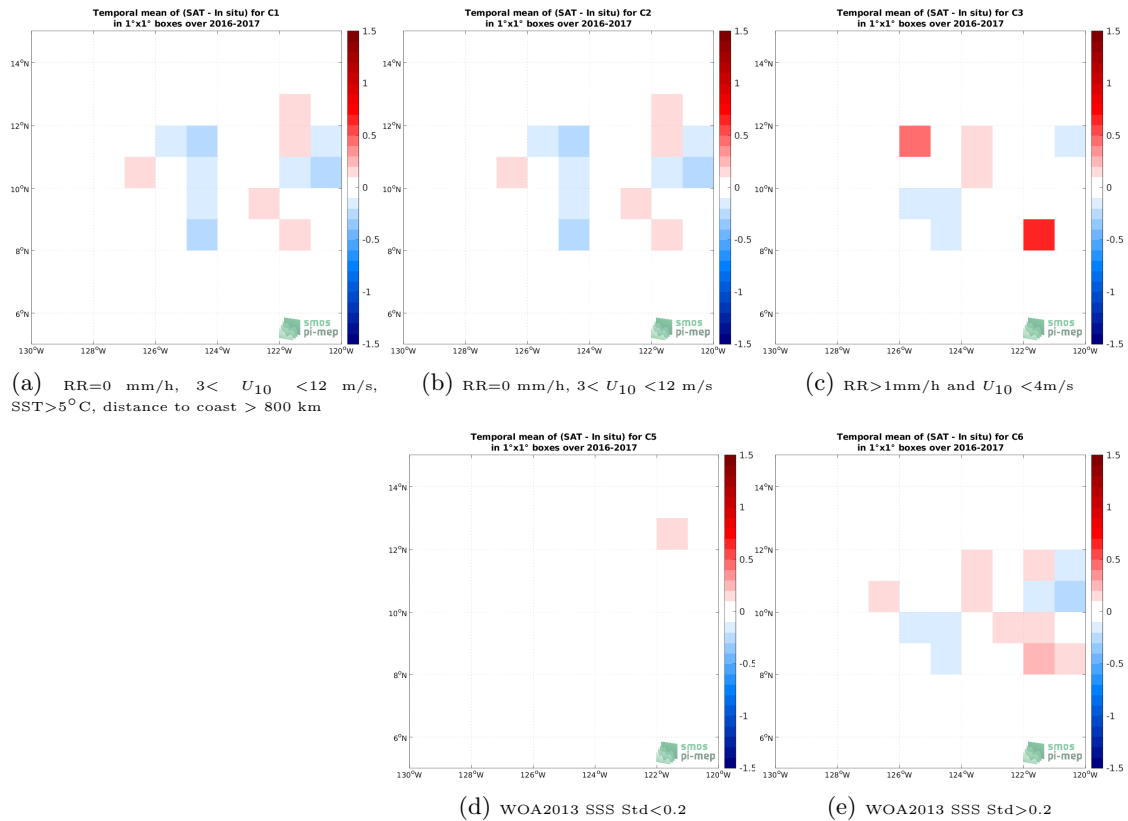
Figure 11: Temporal mean gridded over spatial boxes of size $1° \times 1°$ of ΔSSS (SMAP SSS L3 v4 - Monthly (RSS) - Waveglider) for 5 different subdatasets corresponding to:RR=0 mm/h, 3< U_{10} <12 m/s, SST>5°C, distance to coast > 800 km (a), RR=0 mm/h, 3< U_{10} <12 m/s (b), RR>1mm/h and U_{10} <4m/s (c), WOA2013 SSS Std<0.2 (d), WOA2013 SSS Std>0.2 (e).

(a) RR=0 mm/h, 3< U_{10} <12 m/s, SST>5°C, distance to coast > 800 km

(b) RR=0 mm/h, 3< U_{10} <12 m/s

(c) RR>1mm/h and U_{10} <4m/s

(d) WOA2013 SSS Std<0.2
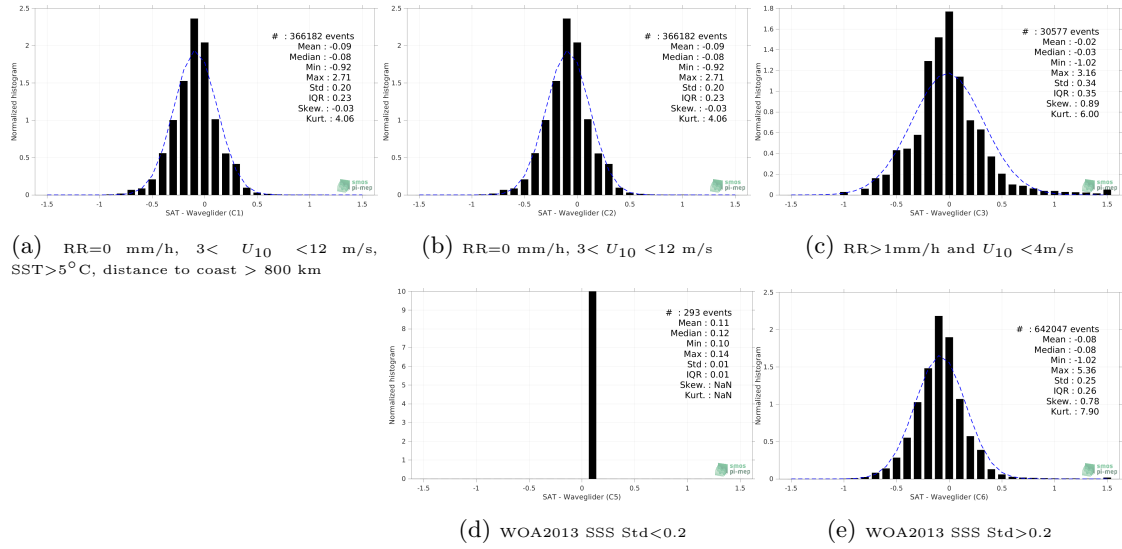
(e) WOA2013 SSS Std>0.2

Figure 12: Normalized histogram of ΔSSS (SMAP SSS L3 v4 - Monthly (RSS) - Waveglider) for 5 different subdatasets corresponding to: RR=0 mm/h, 3< U_{10} <12 m/s, SST>5°C, distance to coast > 800 km (a), RR=0 mm/h, 3< U_{10} <12 m/s (b), RR>1mm/h and U_{10} <4m/s (c), WOA2013 SSS Std<0.2 (d), WOA2013 SSS Std>0.2 (e).

4 Summary

▶ Table 1 shows the mean, median, standard deviation (Std), root mean square (RMS), interquartile range (IQR), correlation coefficient (r^2) and robust standard deviation (Std⋆) of the match-up differences ΔSSS (Satellite - *in situ*) between SMAP SSS L3 v4 - Monthly (RSS) and Waveglider derived over the SPURS 2 Pi-MEP region and for the full satellite product period and for the following conditions:

- all: All the match-up pairs satellite/*in situ* SSS values are used to derive the statistics

- C1: only pairs where RR=0 mm/h, 3< U_{10} <12 m/s, SST>5°C, distance to coast > 800 km

- C2: only pairs where RR=0 mm/h, 3< U_{10} <12 m/s

- C3: only pairs where RR>1mm/h and U_{10} <4m/s

- C5: only pairs where WOA2013 SSS Std<0.2

- C6: only pairs at WOA2013 SSS Std>0.2

- C7a: only pairs with a distance to coast < 150 km.

- C7b: only pairs with a distance to coast in the range [150, 800] km.

- C7c: only pairs with a distance to coast > 800 km.

- C8a: only pairs where SST is < 5°C.

- C8b: only pairs where SST is in the range [5, 15]°C.

29

- C8c: only pairs where SST is $> 15°$C.

- C9a: only pairs where SSS is < 33.

- C9b: only pairs where SSS is in the range [33, 37].

- C9c: only pairs where SSS is > 37.

Table 1: Statistics of ΔSSS (Satellite - Waveglider)

Condition	#	Median	Mean	Std	RMS	IQR	r²	Std*
all	642340	-0.08	-0.08	0.25	0.26	0.26	0.862	0.19
C1	366182	-0.08	-0.09	0.20	0.22	0.23	0.896	0.17
C2	366182	-0.08	-0.09	0.20	0.22	0.23	0.896	0.17
C3	30577	-0.03	-0.02	0.34	0.35	0.35	0.655	0.26
C5	293	0.12	0.11	0.01	0.11	0.01	0.000	0.01
C6	642047	-0.08	-0.08	0.25	0.26	0.26	0.862	0.19
C7a	0	NaN	NaN	NaN	NaN	NaN	NaN	NaN
C7b	0	NaN	NaN	NaN	NaN	NaN	NaN	NaN
C7c	642340	-0.08	-0.08	0.25	0.26	0.26	0.862	0.19
C8a	0	NaN	NaN	NaN	NaN	NaN	NaN	NaN
C8b	0	NaN	NaN	NaN	NaN	NaN	NaN	NaN
C8c	642340	-0.08	-0.08	0.25	0.26	0.26	0.862	0.19
C9a	158669	-0.01	0.02	0.31	0.31	0.27	0.191	0.20
C9b	483671	-0.10	-0.12	0.21	0.24	0.25	0.808	0.18
C9c	0	NaN	NaN	NaN	NaN	NaN	NaN	NaN

▶ Table 2 presents statistics of ΔSSS (Satellite - ISAS) using only ISAS SSS values with PCTVAR<80%.

Table 2: Statistics of ΔSSS (Satellite - ISAS)

Condition	#	Median	Mean	Std	RMS	IQR	r²	Std*
all	642340	-0.04	-0.07	0.14	0.16	0.16	0.953	0.11
C1	366182	-0.04	-0.06	0.13	0.14	0.14	0.957	0.10
C2	366182	-0.04	-0.06	0.13	0.14	0.14	0.957	0.10
C3	30577	-0.08	-0.07	0.15	0.17	0.18	0.866	0.14
C5	293	0.04	0.04	0.00	0.04	0.00	1.000	0.00
C6	642047	-0.04	-0.07	0.14	0.16	0.16	0.953	0.11
C7a	0	NaN	NaN	NaN	NaN	NaN	NaN	NaN
C7b	0	NaN	NaN	NaN	NaN	NaN	NaN	NaN
C7c	642340	-0.04	-0.07	0.14	0.16	0.16	0.953	0.11
C8a	0	NaN	NaN	NaN	NaN	NaN	NaN	NaN
C8b	0	NaN	NaN	NaN	NaN	NaN	NaN	NaN
C8c	642340	-0.04	-0.07	0.14	0.16	0.16	0.953	0.11
C9a	158669	-0.10	-0.11	0.14	0.18	0.20	0.733	0.14
C9b	483671	-0.04	-0.05	0.14	0.15	0.14	0.918	0.11
C9c	0	NaN	NaN	NaN	NaN	NaN	NaN	NaN

▶ Numerical values can be downloaded as csv files for Table 1 and Table 2.

5 More Comparison/Validation Materials

5.1 Comparisons with other satellite products

▶ Table 1 shows the mean, median, standard deviation (Std), root mean square (RMS), interquartile range (IQR), correlation coefficient (r^2) and robust standard deviation (Std*) of the match-up differences ΔSSS (Satellite - Waveglider) between different satellite products and **Waveglider** derived over the SPURS 2 Pi-MEP region considering all match-up pairs satellite/*in situ* SSS values to derive the statistics:

Table 1: Statistics of ΔSSS (Satellite - Waveglider) - All

Satellite products	#	Median	Mean	Std	RMS	IQR	r^2	Std*
smos-l2-v700	260956	0.03	-0.05	0.63	0.63	0.82	0.510	0.58
smap-l2-rss-v5	396499	-0.03	-0.03	0.38	0.38	0.43	0.699	0.32
smap-l2-rss-v5-40km	374248	-0.03	-0.03	0.65	0.66	0.84	0.462	0.63
smap-l2-jpl-v5.0	459190	-0.01	-0.01	0.54	0.54	0.66	0.571	0.49
smos-l3-catds-cpdc-v330-l2q	119418	0.04	0.02	0.70	0.70	0.96	0.439	0.71
smos-l3-catds-cpdc-v335-10d-25km	248204	0.08	0.09	0.31	0.32	0.38	0.790	0.29
smos-l3-catds-cpdc-v335-1m-25km	249818	0.09	0.10	0.29	0.30	0.37	0.821	0.27
smos-l3-catds-locean-v7-9d	597814	-0.01	0.01	0.27	0.27	0.32	0.834	0.24
smos-l3-catds-locean-v7-18d	624774	-0.01	0.01	0.26	0.26	0.32	0.855	0.24
smos-l3-bec-v2-9d	267987	0.40	0.44	0.38	0.58	0.56	0.759	0.41
smap-l3-rss-v4-8dr	642340	-0.08	-0.09	0.26	0.27	0.27	0.854	0.20
smap-l3-rss-v4-1m	642340	-0.08	-0.08	0.25	0.26	0.26	0.862	0.19
smap-l3-rss-v5-8dr	640901	-0.08	-0.10	0.26	0.28	0.28	0.855	0.20
smap-l3-rss-v5-1m	642340	-0.09	-0.10	0.25	0.27	0.27	0.858	0.20
smap-l3-jpl-v5.0-8dr	642340	0.02	0.03	0.25	0.25	0.27	0.855	0.20
smap-l3-jpl-v5.0-1m	642340	0.01	0.03	0.24	0.24	0.26	0.865	0.19
smos-smap-l4-lops-oi-v1-7d	249818	0.04	0.05	0.26	0.26	0.29	0.852	0.21
smos-l4-cmems-cnr-v1-1w	268967	0.04	0.05	0.25	0.25	0.24	0.872	0.18
smos-l4-cmems-cnr-v1-1m	268967	0.04	0.05	0.26	0.26	0.30	0.865	0.22
cci-l4-esa-merged-oi-v3.2-7dr	249737	0.00	0.02	0.27	0.27	0.29	0.835	0.22
cci-l4-esa-merged-oi-v3.2-30dr	246340	0.02	0.04	0.27	0.28	0.28	0.838	0.21
smap-l4-iprc-oi-v1-7d	268967	0.10	0.12	0.26	0.28	0.24	0.859	0.18
smap-l4-iprc-oi-v1-1m	268967	0.10	0.12	0.26	0.29	0.29	0.848	0.22

▶ Table 2 is similar to Table 1 but considering only match-up pairs where RR=0 mm/h, $3< U_{10} <12$ m/s, SST>5°C, distance to coast > 800 km.

Table 2: Statistics of ∆SSS (Satellite - Waveglider) - C1

Satellite products	#	Median	Mean	Std	RMS	IQR	r^2	Std⋆
smos-l2-v700	158579	0.05	0.01	0.54	0.54	0.72	0.546	0.52
smap-l2-rss-v5	264439	-0.04	-0.03	0.35	0.35	0.40	0.718	0.30
smap-l2-rss-v5-40km	257496	-0.03	-0.03	0.63	0.63	0.82	0.473	0.61
smap-l2-jpl-v5.0	273510	-0.01	0.00	0.48	0.48	0.62	0.586	0.46
smos-l3-catds-cpdc-v330-l2q	66522	0.09	0.09	0.61	0.62	0.92	0.456	0.69
smos-l3-catds-cpdc-v335-10d-25km	135785	0.05	0.05	0.27	0.27	0.36	0.829	0.27
smos-l3-catds-cpdc-v335-1m-25km	136214	0.07	0.07	0.24	0.25	0.37	0.860	0.28
smos-l3-catds-locean-v7-9d	342202	-0.03	-0.02	0.23	0.23	0.29	0.863	0.22
smos-l3-catds-locean-v7-18d	358265	-0.05	-0.03	0.22	0.22	0.28	0.884	0.20
smos-l3-bec-v2-9d	148487	0.30	0.35	0.32	0.48	0.47	0.815	0.33
smap-l3-rss-v4-8dr	366182	-0.07	-0.09	0.21	0.23	0.23	0.892	0.17
smap-l3-rss-v4-1m	366182	-0.08	-0.09	0.20	0.22	0.23	0.896	0.17
smap-l3-rss-v5-8dr	365372	-0.08	-0.10	0.22	0.24	0.24	0.891	0.18
smap-l3-rss-v5-1m	366182	-0.09	-0.10	0.21	0.23	0.24	0.893	0.18
smap-l3-jpl-v5.0-8dr	366182	0.03	0.01	0.20	0.20	0.24	0.895	0.18
smap-l3-jpl-v5.0-1m	366182	0.01	0.01	0.20	0.20	0.24	0.900	0.18
smos-smap-l4-lops-oi-v1-7d	136214	0.01	0.02	0.21	0.21	0.24	0.900	0.17
smos-l4-cmems-cnr-v1-1w	149366	0.03	0.02	0.18	0.19	0.22	0.921	0.16
smos-l4-cmems-cnr-v1-1m	149366	0.01	0.02	0.19	0.19	0.28	0.915	0.21
cci-l4-esa-merged-oi-v3.2-7dr	136103	-0.02	-0.01	0.21	0.21	0.26	0.893	0.20
cci-l4-esa-merged-oi-v3.2-30dr	133328	0.00	0.01	0.21	0.21	0.25	0.897	0.19
smap-l4-iprc-oi-v1-7d	149366	0.10	0.11	0.19	0.22	0.21	0.916	0.15
smap-l4-iprc-oi-v1-1m	149366	0.10	0.10	0.21	0.23	0.27	0.901	0.20

▶ Numerical values can be downloaded as csv files for Table 1 and Table 2.

▶ Figures using numerical values of Table 1 sorted by MEDIANS, MEANS, IQR, RMS, STD, R2 are also provided.

▶ Figures using numerical values of Table 2 sorted by MEDIANS, MEANS, IQR, RMS, STD, R2 are also provided.

Caution has to be made in the interpretation of the "ranking" between different satellite products in particular when looking at the dispersion parameters like the standard deviation (STD), or the interquartile range (IQR). Keep in mind that low spatial and/or temporal resolution satellite SSS products tend to have lower dispersions than products at higher resolutions. For example, a level 2 (swath) product of a specific sensor will always have more dispersion than level 3 or 4 products where spatial and temporal averaging tend to reduce the instrumental noise and potential small scale variability. In general, products at $1° \times 1°$ spatial resolution have lower dispersion than products at $0.25° \times 0.25°$. Same result applies for monthly products compared to daily products.

5.2 Statistics derived for the different *in situ* databases

▶ Table 1 shows the mean, median, standard deviation (Std), root mean square (RMS), interquartile range (IQR), correlation coefficient (r^2) and robust standard deviation (Std⋆) of the match-up differences ∆SSS (Satellite - *in situ*) between **SMAP SSS L3 v4 - Monthly (RSS)** and all the available *in situ* datasets derived over the SPURS 2 Pi-MEP region and for the full satellite product period and considering all match-up pairs satellite/*in situ* SSS values to derive

the statistics:

Table 1: Statistics of ΔSSS (Satellite - *in situ*)

in situ database	#	Median	Mean	Std	RMS	IQR	r²	Std*
argo	3407	-0.06	-0.06	0.23	0.23	0.27	0.826	0.20
tsg-samos	14472	-0.10	-0.38	0.67	0.77	1.00	0.346	0.51
drifter	124214	-0.07	-0.07	0.28	0.29	0.29	0.697	0.21
snake	3428541	-0.04	-0.02	0.40	0.40	0.35	0.443	0.26
saildrone	9218	-0.09	-0.08	0.22	0.23	0.21	0.320	0.15
waveglider	642340	-0.08	-0.08	0.25	0.26	0.26	0.862	0.19
seaglider	73542	-0.04	-0.07	0.24	0.25	0.27	0.860	0.19

▶ Table 2 is similar to Table 1 but considering only match-up pairs where RR=0 mm/h, $3 < U_{10} < 12$ m/s, SST>5°C, distance to coast > 800 km.

Table 2: Statistics of ΔSSS (Satellite - *in situ*)

in situ database	#	Median	Mean	Std	RMS	IQR	r²	Std*
argo	2007	-0.05	-0.05	0.21	0.22	0.26	0.829	0.19
tsg-samos	8122	0.04	0.08	0.24	0.25	0.29	0.715	0.18
drifter	66350	-0.07	-0.08	0.24	0.26	0.28	0.712	0.21
snake	1355328	-0.06	-0.08	0.30	0.31	0.34	0.735	0.25
saildrone	3495	-0.08	-0.07	0.19	0.20	0.22	0.471	0.17
waveglider	366182	-0.08	-0.09	0.20	0.22	0.23	0.896	0.17
seaglider	33071	-0.03	-0.06	0.22	0.23	0.25	0.893	0.17

▶ Numerical values can be downloaded as csv files for Table 1 and Table 2.

References

Abderrahim Bentamy and Denis Croize Fillon. Gridded surface wind fields from Metop/ASCAT measurements. *Int. J. Remote Sens.*, 33(6):1729–1754, March 2012. ISSN 1366-5901. doi: 10.1080/01431161.2011.600348.

Abderrahim Bentamy, Semyon A. Grodsky, James A. Carton, Denis Croizé-Fillon, and Bertrand Chapron. Matching ASCAT and QuikSCAT winds. *J. Geophys. Res.*, 117(C2), February 2012. ISSN 0148-0227. doi: 10.1029/2011JC007479.

Jaqueline Boutin, Y. Chao, W. E. Asher, T. Delcroix, R. Drucker, K. Drushka, N. Kolodziejczyk, T. Lee, N. Reul, G. Reverdin, J. Schanze, A. Soloviev, L. Yu, J. Anderson, L. Brucker, E. Dinnat, A. S. Garcia, W. L. Jones, C. Maes, T. Meissner, W. Tang, N. Vinogradova, and B. Ward. Satellite and In Situ Salinity: Understanding Near-Surface Stratification and Sub-footprint Variability. *Bull. Am. Meterol. Soc.*, 97(8):1391–1407, 2016. ISSN 1520-0477. doi: 10.1175/bams-d-15-00032.1.

Clément de Boyer Montégut, Gurvan Madec, A. S. Fischer, A. Lazar, and D. Ludicone. Mixed layer depth over the global ocean: An examination of profile data and a profile-based climatology. *J. Geophys. Res.*, 109(C12), December 2004. doi: 10.1029/2004jc002378.

Clément de Boyer Montégut, Juliette Mignot, Alban Lazar, and Sophie Cravatte. Control of salinity on the mixed layer depth in the world ocean: 1. General description. *J. Geophys. Res.*, 112(C6), June 2007. ISSN 0148-0227. doi: 10.1029/2006jc003953.

Ralph R. Ferraro. SSM/I derived global rainfall estimates for climatological applications. *J. Geophys. Res.*, 102(D14):16715–16736, 07 1997. doi: 10.1029/97JD01210.

Ralph R. Ferraro, Fuzhong Weng, Norman C. Grody, and Limin Zhao. Precipitation characteristics over land from the NOAA-15 AMSU sensor. *Geophys. Res. Lett.*, 27(17):2669–2672, 2000. doi: 10.1029/2000GL011665.

Fabienne Gaillard, Thierry Reynaud, Virginie Thierry, Nicolas Kolodziejczyk, and Karina von Schuckmann. In Situ-Based Reanalysis of the Global Ocean Temperature and Salinity with ISAS: Variability of the Heat Content and Steric Height. *J. Clim.*, 29(4):1305–1323, February 2016. ISSN 1520-0442. doi: 10.1175/jcli-d-15-0028.1.

Robert J. Joyce, John E. Janowiak, Phillip A. Arkin, and Pingping Xie. CMORPH: A Method that Produces Global Precipitation Estimates from Passive Microwave and Infrared Data at High Spatial and Temporal Resolution. *J. Hydrometeorol.*, 5(3):487–503, June 2004. doi: 10.1175/1525-7541(2004)005⟨0487:camtpg⟩2.0.co;2.

Nicolas Kolodziejczyk, Gilles Reverdin, and Alban Lazar. Interannual Variability of the Mixed Layer Winter Convection and Spice Injection in the Eastern Subtropical North Atlantic. *J. Phys. Oceanogr.*, 45(2):504–525, Feb 2015. ISSN 1520-0485. doi: 10.1175/jpo-d-14-0042.1.

Christian Kummerow, Y. Hong, W. S. Olson, S. Yang, R. F. Adler, J. McCollum, R. Ferraro, G. Petty, D-B. Shin, and T. T. Wilheit. The Evolution of the Goddard Profiling Algorithm (GPROF) for Rainfall Estimation from Passive Microwave Sensors. *J. Appl. Meteorol.*, 40(11): 1801–1820, 2001. doi: 10.1175/1520-0450(2001)040⟨1801:TEOTGP⟩2.0.CO;2.

Thomas Meissner, Frank J. Wentz, and David M. Le Vine. The Salinity Retrieval Algorithms for the NASA Aquarius Version 5 and SMAP Version 3 Releases. *Remote Sens.*, 10(7):1121, jul 2018. doi: 10.3390/rs10071121.